Prepared for submission to JHEP NITS-PHY-2014008

# Nonplanar On-shell Diagrams and Leading Singularities of Scattering Amplitudes

**Baoyi Chen, Gang Chen[1], Yeuk-Kwan E. Cheung[2], Yunxuan Li, Ruofei Xie, Yuan Xin**

*Department of Physics, Nanjing University*
*22 Hankou Road, Nanjing 210093, P. R. China*

*E-mail:* gang.chern@gmail.com, cheung@nju.edu.cn

arXiv:1411.3889v1 [hep-th] 14 Nov 2014

Abstract: The leading singularities encode important information of the scattering amplitudes and can be used in the construction of loop-level amplitudes. In this paper we study systematically the on-shell diagrams for the leading singularities of nonplanar amplitudes in $\mathcal{N} = 4$ super Yang-Mills (SYM) theory. In particular we prove that a nonplanar leading singularity can be constructed by employing Britto–Cachazo–Feng–Witten (BCFW) bridges together with the $U(1)$ decoupling relations of three and four point tree-level amplitudes. Accordingly we obtain the BCFW-bridge decomposition chain and permutation rules for any nonplanar leading singularities, leading in a straightforward way to the "d*log* form." The BCFW decomposition chain encodes the geometrical information in the Grassmannian submanifolds corresponding to each nonplanar on-shell diagram. The integrands of nonplanar "top-forms" can also be obtained from the BCFW data. To calculate the leading singularities explicitly, we introduce a canonical ordering of BCFW-bridge decompositions and obtain the recursion relations for all poles, arriving at the *BCFW-constructed form* for the amplitude. We, inspired by the BCFW recursion relation for the underlying tree-level diagrams, extend it to the loop level and non-planarity. Utilizing all three forms of nonplanar amplitudes constructed by us, one can fully decompose a nonplanar leading singularity, obtain the geometrical data, and explicitly calculate the amplitudes in an extremely efficient manner.

Keywords: Nonplanar Amplitudes, Non-positive Grassmannians, N=4 Super Yang-Mills, Unitarity Cuts, BCFW

[1]Corresponding author
[2]Corresponding author

## Contents


**1 Introduction** **1**

**2 Scattering amplitudes: BCFW decomposition and d*log* form** **3**

2.1 Unglued diagram and marked permutation 4

2.2 From permutations to BCFW decompositions 5

2.3 The d*log* form 9

**3 Scattering amplitudes: the *Top–form*** **10**

3.1 Geometry and the BCFW-Bridge Decomposition 11

3.2 The integrand of the top-form 14

**4 Scattering amplitude: the *BCFW constructed form*** **20**

4.1 Marked permutations, pole types and the canonical order 22

4.2 Amplitude recursion relation under the canonical order 26

4.3 Examples 30

**5 conclusion and outlook** **36**

**A BCFW-bridge decomposition to three basic types of diagrams** **38**

**B Geometry and Permutation** **45**


## 1 Introduction

Scattering amplitudes are of profound importance in high energy physics describing the interactions of fundamental forces and elementary particles. The scattering ampli-

tudes are widely studied for $\mathcal{N}=4$ super Yang-Mills theory and QCD. At tree level, BCFW recursion relations [1–4] can be used to calculate n-point amplitudes efficiently. Unitarity cuts [5–7] and generalized unitarity cuts [8–15] combined with BCFW for the rational terms work well at loop level [16–21].

Leading singularities [22] are closely related to the unitarity cuts of loop-level amplitudes. For planar diagrams in $\mathcal{N}=4$ super Yang-Mills [23, 24], the leading singularities are invariant under Yangian symmetry [25–28], which is a symmetry combining conformal symmetry and dual conformal symmetry [29–33]. The leading singularity can also be used in constructing one-loop amplitudes by taking this as the rational coefficients of the scalar box integrals. Extending this idea to higher loop amplitudes are reported in [10, 34–36].

A leading singularity can be viewed as a contour integral over a Grassmannian manifold [37–42]. This expression of the leading singularity keeps many symmetries, in particular, the Yangian symmetry, cyclic and parity symmetries, manifest. On the one hand this new form makes the expression of amplitudes simple and hence easy to calculate. On the other hand it is related to the central ideas in algebraic geometry: Grassmmannian, stratification, algebraic varieties, toric geometry, and intersection theory etc.. For leading singularities of the planar amplitudes in $\mathcal{N}=4$ super Yang-Mills (SYM) , Arkani-Hamed et al [43] proposed using positive Grassmannian to study them along with the constructions of the bipartite on-shell–all internal legs are put on shell–diagrams [44].

Top-forms and the d"*log*" forms of the Grassmannian integrals are systematically studied for planar diagrams. Each on-shell diagram corresponds to a Yangian invariant, as shown in [31] at tree level and [32, 33, 45] at loop level. (See also [46, 47] for earlier works and [48–62] for a sample of interesting developments thereafter, and [63–75] for a sample of reviews and a new book [76].)

We report, in this paper, our detailed and systematic studies of the nonplanar on-shell diagrams. We prove that a nonplanar on-shell diagram of the leading singularity of a given amplitude can be decomposed into an all-line disconnected diagram–the identity–by removing BCFW-bridges and applying U(1) decoupling relation of the four- and three-point amplitudes. We first construct the chain of BCFW-decompositions for general nonplanar on-shell diagrams. During this process we obtain the unglued diagram by cutting an internal line. We prove any unglued diagrams can be categorized into three distinct classes which can be subsequently turned into identity utilizing crucially the permutation relation of generalized Yangian Invariants [77]. Following the

BCFW decomposition chain, it is then straightforward to write down the d*log* form for the leading singularity of an on-shell diagram. This construction is presented in Section 2.

We then proceed to study the geometry of the leading singularities. We are interested in the constraints encoded in the Grassmannian manifolds and how these constraints determine the integration contours in the top-forms. As the cyclic order is destroyed by non-planarity the integrand of Grassmannian integral also needs to be constructed from scratch. To achieve the above goals we attach non-adjacent BCFW-bridges to the planar diagrams and observe how the integrands and the C-matrices transform. Further we can construct the top-form including both integrand and integration contour of any nonplanar leading singularity by attaching BCFW-bridges to the identity diagram in the reverse order of the BCFW decomposition chain from the previous section. This construction is presented in Section 3

Although the routes to arrive at the identity through BCFW decompositions can be found by our recipe described in Section 2 to facilitate the explicit computation of a leading singularity, we choose a particular integration parameter and fix an integration order to simplify the integrals. We define a canonical ordering such that, in general, a pole will emerge upon one step of BCFW-bridge removal, presented in Section 4. Our construction using the on-shell diagrams is inspired by tree-level BCFW recursion relation [1–4], but extending it to leading singularities arisen in loop level amplitudes, noticing that the poles we obtained in the canonical orders are analogous to the on-shell propagators and three-vertices in BCFW recursion relations of tree level Feynman diagrams.

## 2 Scattering amplitudes: BCFW decomposition and d*log* form

Leading singularities refer to Yang-Mills scattering amplitudes in which all internal momentum integrations are fixed by delta functions. They occur upon gluing a chain of tree level amplitudes to form loops. As the tree-level amplitudes in $\mathcal{N} = 4$ can be casted into the on-shell bipartite diagrams, the on-shell diagrams for leading singularities–be it planar or nonplanar–can then be constructed directly by gluing the corresponding tree-level on-shell diagrams. On-shell diagrams are bipartite graphs with all internal lines on-shell. The advantage of studying on-shell diagrams as supposed to the conventional approach of computing Feynman diagrams is the elimination of gauge redundancies. [78] An equivalence class of planar on-shell diagrams are associated with

a certain *permutation* [43]. Permutations therefore encode all physical information of the associated on-shell graphs, and in particular the BCFW decompositions [1–4].

In non-planar cases the BCFW bridge decomposition is still a powerful way for calculating the scattering amplitudes and for analyzing the Grassmannian geometry as we shall see. To obtain the series of BCFW bridge decompositions on the one loop leading singularities, we cut an internal loop line of the on-shell nonplanar graph resulting in an unglued planar diagram with two marked points as shown in Fig. 1. The unglued diagram is specified by the order of their external legs, the "permutations." Bridge decomposing the unglued diagram can lead to three different classes of irreducible skeleton graphs as depicted in Fig. 3. The crucial step then is to make use of the permutation relation of the general Yangian Invariants found in [77] to convert any nonplanar elements into planar ones and further reducing the skeleton graphs into the identity. With the chain of BCFW decomposition in hand it is then straightforward to write down the "d*log*" form for the leading singularities of the nonplanar on-shell diagrams. In this section, we will introduce a systematic way of finding the BCFW bridge decomposition chain from the marked permutations [1] of the unglued planar diagrams upon a single cut and construct the "d*log*" form from the chain.

### 2.1 Unglued diagram and marked permutation

The series of BCFW bridge decompositions for planar diagrams are readily obtained from the permutations of the external legs. However, permutations of the external legs are not well defined in nonplanar cases, unless we can transform nonplanar leading singularities into planar ones. Fortunately, this can be realized in the on-shell diagrams with the newly discovered permutation relation of the generalized Yangians [77]. To this end we first define two key operations on the nonplanar graphs in order to obtain the unglued diagrams, and then proceed to describe how to obtain the permutations of the unglued diagrams from the tree-level subgraphs.

First we explain how to transform nonplanar leading singularities into planar ones. Since in on-shell diagrams all lines–be it internal or external–are on-shell, helicity and momentum can both be defined. There are no distinctions between these two types of lines. Thus we can define a "*cut*" operation on an internal loop line of the on-shell nonplanar graph resulting in an unglued planar diagram with two marked points as shown in Fig. 1. The contrary process is then defined as a "*glue*" operation. By

[1] Marked permutations refer to permutations with two end points treated specially–the two points are allowed to marked to themselves or to each other.

applying a *cut*, we turn an unlabeled internal on-shell line into two labeled external on-shell lines. To retrieve the original nonplanar diagram, one only need to integrate the cut line momenta in the amplitude expression, which is a *glue*.

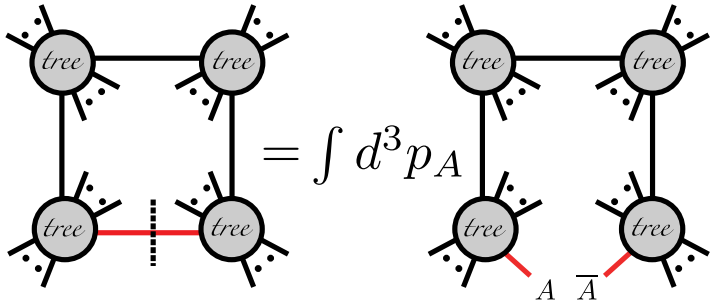


**Figure 1**. Cutting a loop internal line of an 1-loop leading singularity converts it into an unglued graph with a pair of marked external lines

Second, the "*marked permutation*" of the unglued diagram can be obtained directly from the permutations of the four tree-level subgraphs by merging two subgraphs' permutations one by one as follows.

$$\begin{pmatrix} a_1 & \cdots & a_i & \cdots & a_{n-1} & a_n \\ \downarrow & \downarrow & \downarrow & \downarrow & \downarrow & \downarrow \\ \sigma(a_1) & \cdots & a_n & \cdots & \sigma(a_{n-1}) & \sigma(a_n) \end{pmatrix} \text{ and } \begin{pmatrix} b_1 & b_2 & \cdots & b_j & \cdots & b_m \\ \downarrow & \downarrow & \downarrow & \downarrow & \downarrow & \downarrow \\ \sigma(b_1) & \sigma(b_2) & \cdots & b_1 & \cdots & \sigma(b_m) \end{pmatrix}$$

can be glued to form

$$\begin{pmatrix} a_1 & \cdots & a_i & \cdots & a_{n-1} & b_2 & \cdots & b_j & \cdots & b_m \\ \downarrow & \downarrow & \downarrow & \downarrow & \downarrow & \downarrow & \downarrow & \downarrow & \downarrow & \downarrow \\ \sigma(a_1) & \cdots & \sigma(b_1) & \cdots & \sigma(a_{n-1}) & \sigma(b_2) & \cdots & \sigma(a_n) & \cdots & \sigma(b_m) \end{pmatrix}$$

according to $\sigma^{-1}(a_1) \to \sigma(b_1), \sigma^{-1}(b_1) \to \sigma(a_1)$ where we take $a_n$ and $b_1$ as the gluing lines without loss of generality.

In the following discussions of this section, we set out from the unglued diagram's marked permutation to construct the BCFW bridge decomposition chain for any one loop nonplanar leading singularity, keeping it in mind that we should *glue* back the *cut* line finally.

### 2.2 From permutations to BCFW decompositions

In this subsection, we derive the BCFW-bridge decomposition chain from the permutation of the unglued diagram. First we perform BCFW bridge decompositions on the

unglued diagram according to marked permutation, leaving the cut lines untouched. Upon the removal of all adjacent bridges, we will arrive at three categories of skeleton diagrams, noticing that the category type is invariant under the BCFW bridge decomposition. Next for each category of skeleton diagram we construct a specific recipe to decompose it to identity.

**From unglued diagram to skeleton diagram** All unglued diagrams can be categorized into three groups depending on the permutations of the two cut lines, denoted as $A$ and $\bar{A}$,

**(1)** $\sigma_1(A) \neq \bar{A}$ && $\sigma_1(\bar{A}) \neq A$;

**(2)** $\sigma_2^a(A) = \bar{A}$ && $\sigma_2^a(\bar{A}) \neq A$, or $\sigma_2^b(\bar{A}) = A$ && $\sigma_2^b(A) \neq \bar{A}$;

**(3)** $\sigma_3(A) = \bar{A}$ && $\sigma_3(\bar{A}) = A$.

To decompose an unglued diagram, the first step is the full removal of two types of adjacent bridges on the target diagram: the *white-black bridge* and the *black-white bridge* as shown in Fig.2. The changes to the permutation after removing either of them are, respectively, $\sigma \to \sigma' = Z_2(k, k+1) \cdot \sigma$ and $\sigma \to \sigma' = Z_2(\sigma^{-1}(k), \sigma^{-1}(k+1)) \cdot \sigma$, where $Z_2(k, k+1)$ is a $Z_2$ permutation between line $k$ and $k+1$[43]. For an unglued

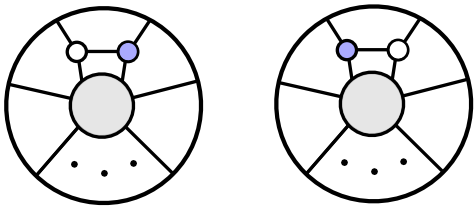

**Figure 2**. white-black bridges and black-white bridges

diagram arisen from a nonplanar leading singularity, the cut line should not be involved in BCFW bridge decompositions as the pair of marked lines are to be glued back eventually. Thus we should restrict the set of allowed BCFW bridge decompositions to those preserving the two marked legs. By following this restriction, the group our target unglued diagram originally belongs to will not alter during bridge decompositions.

Due to the existence of nonadjacent bridges, an unglued diagram cannot be fully decomposed and will pause at a certain diagram. We prove in Appendix A that after removing all BW- and WB- bridges the three groups of unglued diagrams will fall into *External line pair*, *Black-White Chain* and *Box Chain* respectively. The three

categories are named after their general patterns as shown in Fig. 3. We refer to any diagram belonging to the above three categories as the *"skeleton diagram"*, naming after its skinny looks. As long as we can fully decompose all three skeleton diagrams, it is then direct to obtain the complete decomposition chain of any unglued diagram.

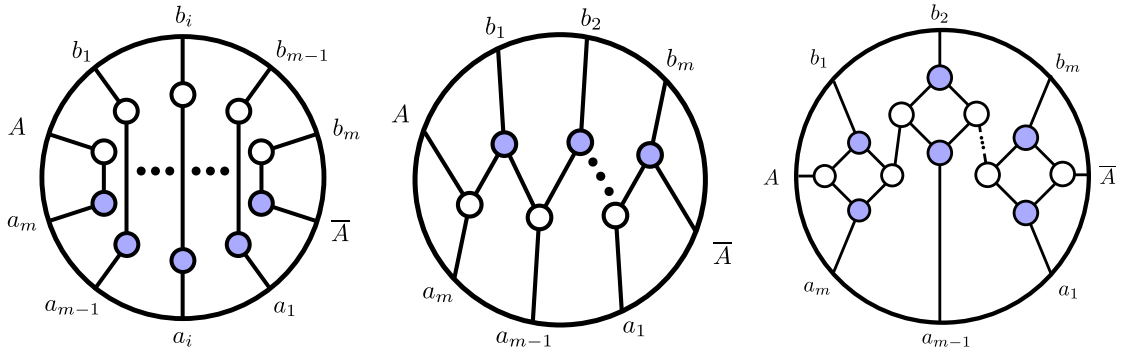


(a) External line Pair (b) Black-White Chain (c) Box Chain

**Figure 3**. Skeleton Diagrams

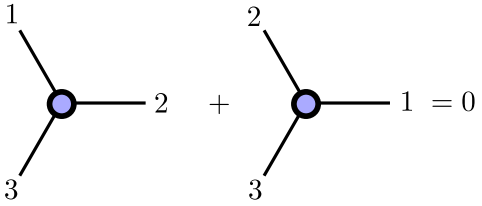


**Figure 4**. $U(1)$ decoupling relation of 3-point amplitudes.

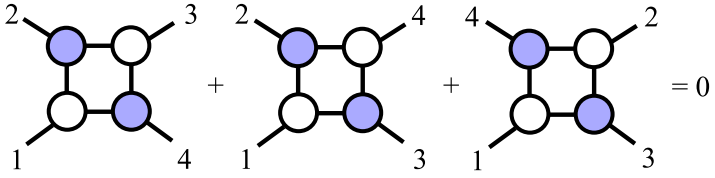


**Figure 5**. $U(1)$ decoupling relation of 4-point amplitudes

**From skeleton diagram to identity**

- **External Line Pair:** Most external lines are paired. The external lines next to the internal cut line may also attach to the black/white vertices or be paired with the internal cut line as shown in Fig 3(a). For this type of on-shell diagrams, gluing back the internal lines and removing all pairs will lead to the identity.
- **Black-White Chain:** In this case, white and black vertices are connected together recursively, as shown in Fig 3(b). To further decompose, we use the am-

plitudes relation $\mathcal{A}(a_1, a_2, a_3) = -\mathcal{A}(a_1, a_3, a_2)$ (see Fig 4) to twist one down-leg to up-leg. Then an adjacent bridge will appear. By removing the new appeared BCFW bridge, the diagram is unfolded into a planar diagram. The diagram can then be decomposed to identity according to its permutation [43].

- **Box Chain:** In this case, the diagram is composed by boxes linked to a chain, as shown in Fig 3(c). Using the $U(1)$ decoupling relation [79] of the four point amplitudes (see Fig 5), this diagram turns into the sum of two diagrams with adjacent BCFW bridges. The non-adjacent legs of the box will become adjacent under this operation. Performing adjacent BCFW decompositions on both diagrams will unfold the loop and arrive at two planar diagrams, which can be decomposed to identity.

We have explained how to obtain the chain of BCFW-bridge decompositions for a general n-point nonplanar diagram. We now summarize the above strategy:

**Summary of the Strategy**

- For a non-planar 1-loop on-shell diagram, one cut a loop line and obtain an unglued loop diagram.
- Perform adjacent BCFW bridge decompositions on the unglued diagram, including both black-white and white-black bridges, until it arrives at a certain "skeleton diagram".
- For the Black-White Chain, twist one non-planar external leg and remove one generated adjacent BCFW bridge to unfold the loop. For Box Chain, use $U(1)$ decoupling relation [79] of the four point amplitudes to turn the diagram into the sum of two diagrams with adjacent BCFW bridges. Remove two generated adjacent BCFW bridges to unfold the loop for each diagram.
- Glue back the cut line in the remaining graph and decompose the diagram to identity.

By now we have obtained the BCFW bridge decomposition chain for general one-loop nonplanar leading singularities. We would like to stress that our strategy can be extended in a straightforward way to the higher loops. We now explain how to obtain the d*log* form from the chain of BCFW-bridge decompositions. This is in exact analogy to the planar cases [43].

### 2.3 The d*log* form

According to the BCFW-decomposition chains and $U(1)$ decoupling relations in the previous discussion, we are finally able to write down the d*log* forms of nonplanar leading singularities.

Here we denote a complete BCFW bridge decomposition chain as $\mathcal{D}$ and the d*log* form obtained from the chain as $\mathcal{A}(\mathcal{D})$.

- In the external line pair case, the on-shell diagram is turned into identity by subsequently removing BCFW-bridges. Thus the amplitude only depends on the decomposition chain:

$$\mathcal{A} = \mathcal{A}(\mathcal{D}) \tag{2.1}$$

- In the black-white pair case, we should apply the $U(1)$ decoupling relation of 3-point amplitude on the skeleton graph. This will attach a minus sign to the amplitude:

$$\mathcal{A} = -\mathcal{A}(\mathcal{D}) \tag{2.2}$$

- In the box chain case, we should add up the two terms resulting from the $U(1)$ decoupling relation of 4-point amplitude:

$$\mathcal{A} = -\mathcal{A}(\mathcal{D}_1) - \mathcal{A}(\mathcal{D}_2) \tag{2.3}$$

The expression of $\mathcal{A}(\mathcal{D})$ has been studied in [43]. Here we present a short review of it:

After removing one BCFW bridge $\mathcal{B}(i_I, j_I; \alpha_I)$ with leg $i_I, j_I$ attached to white and black vertices respectively, the amplitudes will transform as

$$\mathcal{A}_n^k(\cdots i_I, \cdots j_I, \cdots) = \int \frac{d\alpha_I}{\alpha_I} \mathcal{A}_n^k(\cdots \hat{i}_I, \cdots \hat{j}_I, \cdots), \tag{2.4}$$

Then $\mathcal{A}(\mathcal{D})$ is obtained by removing BCFW bridges subsequently.

$$\mathcal{A}(\mathcal{D}) = \mathcal{A}_n^k = \int_{C_\sigma} \frac{d\alpha_1}{\alpha_1} \wedge \cdots \wedge \frac{d\alpha_d}{\alpha_d} \delta^{k\times 2}(C \cdot \tilde{\lambda}) \delta^{(n-k)\times 2}(\lambda \cdot C_\perp^\top) \delta^{k\times 4}(C \cdot \tilde{\eta}) \tag{2.5}$$

The matrix $C$ and $C_\perp^\top$ can be obtained from

$$\begin{aligned} C &= C_0\mathcal{B}(i_1, j_1; \alpha_1)\cdots\mathcal{B}(i_{2n-4}, j_{2n-4}; \alpha_{2n-4}) \\ C_\perp^\top &= \mathcal{B}(i_{2n-4}, j_{2n-4}; -\alpha_{2n-4})\cdots\mathcal{B}(i_1, j_1; -\alpha_1)C_{0\perp}^\top \end{aligned} \tag{2.6}$$

where

$$\mathcal{B}(i_I, j_I; \alpha_I) = \begin{array}{c} \\ i_I \end{array} \begin{array}{c} \begin{array}{cccccccc} & & & & & j_I & & \end{array} \\ \begin{pmatrix} 1 & 0 & \cdots & 0 & \cdots & 0 & \cdots & 0 \\ 0 & 1 & \cdots & 0 & \cdots & 0 & \cdots & 0 \\ \vdots & \vdots & \ddots & 0 & \cdots & 0 & \cdots & 0 \\ 0 & 0 & 0 & 1 & \cdots & \alpha_I & \cdots & 0 \\ \vdots & \vdots & \vdots & \vdots & \ddots & 0 & \cdots & 0 \\ 0 & 0 & 0 & 0 & 0 & 1 & \cdots & 0 \\ \vdots & \vdots & \vdots & \vdots & \vdots & \vdots & \ddots & 0 \\ 0 & 0 & 0 & 0 & 0 & 0 & \cdots & 1 \end{pmatrix} \end{array}.$$

and the $C_0$ and $C_{0\perp}$ are the Grassmannian matrices of the identity.

In the above discussions we show that any nonplanar leading singularity can be decomposed into identity by BCFW bridge decompositions and $U(1)$ decoupling relation. We also construct the d*log* form according to the decomposition chain. This finally enables us to analyze the geometry of the nonplanar leading singularities and to calculate any one-loop amplitudes explicitly. We shall discuss these aspects in the following sections.

## 3 Scattering amplitudes: the *Top–form*

Through the BCFW bridge decompositions we obtain the d*log* form characterized by the bridge parameters. The d*log* form can be viewed as an explicit parameterization of a more general integration over the Grassmannian manifold, which is invariant under the $GL(k)$ transformations. The invariant form, known as the "top-form," for planar diagrams has been constructed in [43]. In this section, we construct the top-form for the nonplanar leading singularities.

For planar diagrams, the top-form manifests the Yangian symmetry: the leading singularities can be written as multidimensional residues in the Grassmannian manifold

$\mathcal{G}(k,n)$,

$$\mathcal{T}_n^k = \oint_{C\subset\Gamma} \frac{d^{k\times n}C}{vol(GL(k))} \frac{\delta^{k\times 4}(C\cdot\widetilde{\eta})}{f(C)} \delta^{k\times 2}(C\cdot\widetilde{\lambda})\delta^{2\times(n-k)}(\lambda\cdot C_\perp^\top), \tag{3.1}$$

where $\Gamma$ is a sub-manifold of $\mathcal{G}(k,n)$. $\Gamma$ is constrained by a set of linear relations among the columns of $C$–certain minors of $C$ be zero. As any function of the minors of $C$, $f(C)$, has the scaling property $f(tC) = t^{k\times n}f(C)$, the d*log* form Eq. 2.5 can be obtained with an appropriate parametrization of $\Gamma$.

To construct the top-form for nonplanar leading singularities, we need to determine the integration contour $\Gamma$ and the integrand $f(C)$. Since the integration contour is constrained by a set of geometrical relations linear in $\alpha$'s, we make use of the BCFW chain we obtained in Section 2 to look for all geometric constraints, fixing $\Gamma$ in the process [2]. Next we will see, with the BCFW approach extended to one-loop, the integrand of the top-form can be calculated by attaching BCFW bridges.

### 3.1 Geometry and the BCFW-Bridge Decomposition

In this subsection we shall introduce the method of searching for geometric constraints in the Grassmannian matrix. Geometric constraints are linear relations among columns of $C$ matrix; and each time we attach a bridge a constraint will be fixed and the linear relations change accordingly.

In the Grassmannian matrix, adding a white-black bridge on external lines $\mathbf{a}$, $\mathbf{b}$ yields a linear transformations of the two columns, $\mathbf{a}$ and $\mathbf{b}$, $\mathbf{a} \longrightarrow \widehat{\mathbf{a}} = \alpha\mathbf{a}+\mathbf{b}$; whereas adding a black-white bridge means $\mathbf{b} \longrightarrow \widehat{\mathbf{b}} = \alpha\mathbf{b}+\mathbf{a}$. We can classify the minors into four sets according to the elements:

1. $(\mathbf{a},\ \mathbf{b}, 1, 2...m_1)^{k_1}$
2. $(\mathbf{a}, 1, 2...m_2)^{k_2}$
3. $(\mathbf{b}, 1, 2...m_3)^{k_3}$
4. $(1, 2, ...m_4)^{k_4}$

where $k_1$ to $k_4$ are the ranks of the minors. Without loss of generality, we shall make $k_1 < m_1 + 2$, $k_2 < m_2 + 1$, $k_3 < m_3 + 1$ and $k_4 < m_4$. We call the minor *complete* if only if adding any other column to the matrix will make the rank increase by one. From now on we shall assume that all the minors in the above sets are complete in the following discussion. In fact, incomplete minors can always be transformed into the

[2] We also present another interesting method , in Appendix B, by gluing planar subgraphs to determine the geometric constraints in leading singularities.

complete ones by adding to the bracket all the necessary elements while keeping the rank unaltered.

Attaching a white-black bridge does not change the rank of minors in *set* 1 since $a$ and $b$ are both in this set. The minors in *set* 2 and *set* 4 remain unaltered since $b$ is excluded from these two sets. $(\alpha\mathbf{a}+\mathbf{b}) \notin span\{\mathbf{b},\mathbf{1},\mathbf{2}...\mathbf{m_3}\}$, thus after adding a white-black bridge the only set with its rank altered is *set* 3. The minors in *set* 3 can generate two new linear relations: $(a,b,1,2...m_3)^{k_3+1}$ and $(1,2...m_3)^{k_3}$. Similarly, upon attaching a black-white bridge, the minors in *set* 2 will become $(a,b,1,2...m_2)^{k_2+1}$ and $(1,2...m_2)^{k_2}$. We have completed the discussion of how constraints alter during each step of bridge decompositions.

Next we turn to attaching bridges starting from the identity with the identity diagram being a matrix with $n-k$ columns of zero vectors. Each time we attach a BCFW bridge, the number of independent geometric constraints will decrease by one. This can be proved through the following procedure. Attaching the bridge (a, b) affects the linear relation involving $\mathbf{b}$. The only exceptions are the relations containing both $a$ and $b$, which will not be affected by the bridge (a, b).

$$(b,1,2...m)^k \longrightarrow \begin{cases} (\mathbf{a},\mathbf{b},1,2...\mathbf{m})^{k+1} \\ (1,2...m)^k \end{cases}$$

If $k=m$, the linear relation $(1,2...m)^k$ does not give rise to any constraint, thus $(a,b,1,2...m)^{k+1}$ has one higher rank than $(b,1,2...m)^k$. The constraints' number is then diminished by one upon attaching the bridge. If $k<m$, the linear relation $(b,1,2...m)^k$ can be decomposed to $(b,1,2...k)^k$ and $(1,2...m)^k$. Consider the relations after attaching the bridge: $(a,b,1,2...m)^{k+1}$ and $(1,2...m)^k$. These two relations are not independent and can be transformed to independent ones: $(a,b,1,2...k)^{k+1}$ and $(1,2...m)^k$. Comparing the constraints between $(b,1,2...k)^k$ and $(a,b,1,2...k)^{k+1}$, the number of constraints is reduced by one upon adding the BCFW bridge.

As an explicit example, we work out $\mathcal{A}_6^3$'s geometry shown in Fig. 6. This diagram becomes planar upon removal of a white-black bridge (1,4). The remaining BCFW bridge decomposition is:

$$(1,2)\to(2,3)\to(3,4)\to(2,3)\to(1,2)\to(3,5)\to(2,6)$$

Linear relations in identity are then:

$$(4)^0,\ (5)^0,\ (6)^0$$

In the Grassmannian matrix, all elements in the three columns are zero. We then

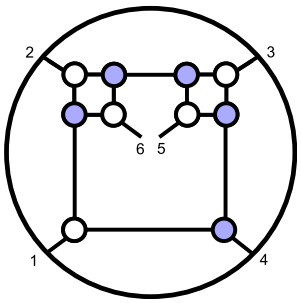


**Figure 6**. The BCFW bridge to open the loop of the diagram.

**Table 1**. The evolution of the geometry constraints under adding BCFW bridges. The first row is the linear relation in the identity diagram and the column on the left represents the bridge decomposition chain.

| | $(4)^0\ (5)^0\ (6)^0$ |
|---|---|
| (2,6) | $(4)^0\ (5)^0\ (2,6)^1$ |
| (3,5) | $(4)^0\ (3,5)^1\ (2,6)^1$ |
| (1,2) | $(4)^0\ (3,5)^1\ (1,2,6)^2$ |
| (2,3) | $(4)^0\ (2,3,5)^2\ (1,2,6)^2$ |
| (3,4) | $(3,4)^1\ (2,3,4,5)^2\ (1,2,6)^2$ |
| (2,3) | $(2,3,4,5)^2\ (1,2,6)^2$ |
| (1,2) | $(3,4,5)^2\ (1,2,6)^2$ |
| (1,4) | $(1,2,6)^2$ |

reconstruct the diagram through attaching BCFW bridges. There are eight bridges needed to construct the nonplanar diagram. Each step will diminish one linear relation. For instance, the first step is adding a white-black bridge on external line 2 and 6, leaving *column* 6 to become $c_6 + \alpha c_2$. The relation $(6)^0$ then becomes $(2,6)^1$. Upon attaching bridge $(3,4)$, relation $(4)^0$ becomes $(3,4)^1$. To keep the minor complete, we should add 5 to the minor $(2,3,5)^2$ and the resulting complete one is $(2,3,4,5)^2$. In the next step of attaching bridge $(2,3)$, the relation $(3,4)^1$ becomes $(2,3,4)^2$, which is already contained in $(2,3,4,5)^2$.

For now we have obtained geometry constraints according to BCFW bridge decomposition chain. During the process, we introduced a method that the constraints are independently and completely represented. The constraints of any graph are almost immediately obtained using our method. Thus the top-form integrations' contour $\Gamma$ is determined.

### 3.2 The integrand of the top-form

For planar diagrams, we can use minors constituted by continuous columns of Grassmannain matrix to represent $f(C)$ (we refer to them as continous minors). But this does not hold for nonplanar diagrams. In this subsection, we will present the expression of $f(C)$ in nonplanar on-shell diagrams. We shall write down the top-form through attaching BCFW bridges (both adjacent and nonadjacent) step by step. If the unglued diagram is a box-chain, U(1) decoupling relation of the four point amplitudes is needed to transform the diagram into the sum of two other diagrams.

**A warmup example** Consider the differences between planar and nonplanar diagrams. When we construct a planar diagram, BCFW bridges are attached merely on adjacent external lines, which does not alter $f(C)$. However, in constructions of nonplanar diagrams attaching bridges will affect $f(C)$ in the top-form in general. To better understand this, we take a nonplanar $\mathcal{A}_4^2$ shown in Fig. **??** as an example.

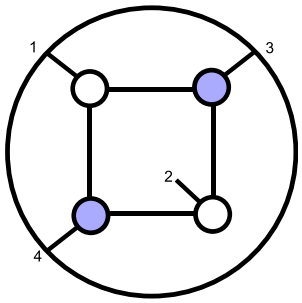


**Figure 7**. Nonplanar diagram $\mathcal{A}_4^2$

Before attaching the nonadjacent bridge $(1,3)$, it is a planar diagram and the top-form is

$$\mathcal{T}_4^2 = \oint_{C\subset\Gamma} \frac{d^{2\times 4}C}{vol(GL(2))} \frac{\delta^{2\times 4}(C\cdot\widetilde{\eta})}{(12)(23)(34)(41)} \delta^{2\times 4}(C\cdot\widetilde{\lambda})\delta^{2\times 2}(\lambda\cdot C_\perp^\top)$$

. The contour $\Gamma$ is around $(23)=0$. We can choose the "gauge" of C matrix as

$$\begin{pmatrix} 1 & 0 & t & c_{14} \\ 0 & 1 & c_{23} & c_{24} \end{pmatrix}.$$

Then we get

$$\oint_{(23)=0} \frac{dt}{t} dc_{14}dc_{23}dc_{24} \frac{\delta^{2\times 4}(C\cdot\widetilde{\eta})}{(12)(34)(41)} \delta^{2\times 4}(C\cdot\widetilde{\lambda})\delta^{2\times 2}(\lambda\cdot C_\perp^\top), \tag{3.2}$$

Integrating over $t$ and attaching the nonadjacent bridge $(1,3)$ yield

$$\widehat{\mathcal{T}_4^2} = \int \frac{d\alpha}{\alpha} dc_{14} dc_{23} dc_{24} \frac{\delta^{2\times 4}(\widehat{C}\cdot\widetilde{\eta})}{((12)(34)(41))\,|_{t=0}} \delta^{2\times 4}(\widehat{C}\cdot\widetilde{\lambda})\delta^{2\times 2}(\lambda\cdot\widehat{C}_\perp^\top),$$

where

$$\widehat{C} = \begin{pmatrix} 1 & 0 & \alpha & c_{14} \\ 0 & 1 & c_{23} & c_{24} \end{pmatrix}.$$

Then we have $\alpha = -(\widehat{23})$, and the top-form becomes

$$\widehat{\mathcal{T}_4^2} = \oint_{\widehat{C}\subset\widehat{\Gamma}} \frac{d^{2\times 4}\widehat{C}}{vol(GL(2))} \frac{-\delta^{2\times 4}(\widehat{C}\cdot\widetilde{\eta})}{(12)(\widehat{23})(34)(41)} \delta^{2\times 4}(\widehat{C}\cdot\widetilde{\lambda})\delta^{2\times 2}(\lambda\cdot\widehat{C_\perp^\top}).$$

Since $c_3 = \widehat{c_3} - \alpha c_1$, we obtain

$$(34) = \frac{(\widehat{34})(12) + (\widehat{23})(14)}{(12)} = \frac{(\widehat{31})(24)}{(12)}.$$

Finally, we rewrite the top-form as

$$\widehat{\mathcal{T}_4^2} = \oint_{\widehat{C}\subset\widehat{\Gamma}} \frac{d^{2\times 4}\widehat{C}}{vol(GL(2))} \frac{-\delta^{2\times 4}(\widehat{C}\cdot\widetilde{\eta})}{(\widehat{23})(\widehat{31})(24)(41)} \delta^{2\times 4}(\widehat{C}\cdot\widetilde{\lambda})\delta^{2\times 2}(\lambda\cdot\widehat{C_\perp^\top}).$$

The difference between top-form of nonplanar diagram $\mathcal{A}_4^2$ and planar diagram $\mathcal{A}_4^2$ is simply a minus sign, which is consistent with the three-point U(1) decoupling relation.

**A general method in obtaining the top-form by attaching a nonadjacent bridge**

In the above example we explicitly obtain the top-form of nonplanar $\mathcal{A}_4^2$ by attaching a nonadjacent BCFW bridge onto a planar diagram. We then move on to study the general cases.

When we attach a bridge $(a,b)$, the linear relation $(b,c_1,c_2,\cdots,c_s)^m$ become:

$$(b,c_1,c_2,\cdots,c_s)^m \to \begin{cases} (a,b,c_1,c_2,\cdots,c_s)^{m+1} \\ (c_1,c_2,\cdots,c_s)^m \end{cases}.$$

The number of constraints is only reduced by one. We may think naively that among the vanishing minors that represent the linear relations, one is removed and the others remain the same—just like the $\mathcal{A}_4^2$ example. However, in general,

- If $m = s = k-1$, $(b, c_1, c_2, \cdots, c_s)^m$ represents only one vanishing minor. There are no vanishing minors generated because $(a, b, c_1, c_2, \cdots, c_s)^k$ and $(c_1, c_2, \cdots, c_s)^s$ are trivial. This is exactly the case we encountered in the warmup example—only one vanishing minor is removed upon attaching a bridge;
- If we don't have $m = s = k-1$, new vanishing minors are generated after attaching a bridge. For example, in $\mathcal{A}_6^3$ case, if the linear relation is $(5,6,1) = 0$ and $(6,1,2) = 0$ and we attach a $(3,1)$ bridge on it, the new constraints is neither $(5,6,1) = 0$ nor $(6,1,2) = 0$ but a new $(3,6,1) = 0$.

To see the transformation of top-form, we can write down the C matrix explicitly:

$$C = \begin{array}{c} \begin{array}{cccccccccccc} a & a_2 & \cdots & a_{k-m} & \cdots & c_1 & \cdots & c_m & b & \cdots & c_s & c_{s+1} & \cdots \end{array} \\ \begin{pmatrix} 1 & 0 & \cdots & 0 & * & & & & t_{1,b} & \dots & t_{1,s} & * & \cdots \\ 0 & 1 & \cdots & 0 & \vdots & & \mathbf{0} & & \vdots & \ddots & \vdots & \vdots & \cdots \\ 0 & 0 & \ddots & 0 & \vdots & & & & \vdots & \cdots & \vdots & \vdots & \cdots \\ 0 & 0 & \cdots & 1 & \vdots & & & & t_{k-m,b} & \dots & t_{k-m,s} & \vdots & \cdots \\ 0 & 0 & \cdots & 0 & \vdots & 1 & & & * & \dots & * & \vdots & \cdots \\ 0 & 0 & \cdots & 0 & \vdots & & \ddots & & \vdots & \ddots & \vdots & \vdots & \dots \\ 0 & 0 & \cdots & 0 & * & & & 1 & * & \dots & * & * & \dots \end{pmatrix} \end{array}. \tag{3.3}$$

Since the rank of matrix $(c_1 \cdots c_s)$ is m, we can choose a proper gauge to fix $C$ into Eq 3.3. Here, $t_{i,j}$ is chosen to be a set of parameters for contour integral around $\Gamma$ and $t_{i,j} = 0$ in $\Gamma$. Attaching the bridge $(a, b)$

$$\widehat{\mathcal{T}_n^k} = \int \frac{d\alpha}{\alpha} \wedge \mathcal{T}_n^k = \int \frac{d\alpha}{\alpha} \oint_\Gamma \frac{d^{k\times(n-k)}C}{f(C)} \delta(\overline{C}),$$

where $\delta(\overline{C})$ represent $\delta(\overline{C} \cdot \widetilde{\eta}) \delta^{k\times 2}(\overline{C} \cdot \widetilde{\lambda}) \delta^{2\times(n-k)}(\lambda \cdot \overline{C}^\perp)$, and $\overline{C}$ is the matrix replacing $t_{1,b}$ by $\alpha + t_{1,b}$ in C. There is a pole at $t_{1,b} = (b, a_2 \cdots a_{k-m}, c_1 \cdots c_m) = 0$. Then, according to C in Eq. 3.3,

$$\widehat{\mathcal{T}_n^k} = \int \frac{d\alpha}{\alpha} \oint_\Gamma \frac{dt_{1b}}{t_{1b}} \frac{d^{k\times(n-k)-1}C}{\overline{f}(C)} \delta(\overline{C}),$$

where $\overline{f}(C) = \frac{f(C)}{t_{1,b}}$. Integrating around the circle of $t_{1,b}$ yields

$$\widehat{\mathcal{T}_n^k} = \oint_{\widehat{\Gamma}} \frac{d\alpha}{\alpha} \frac{d^{k\times(n-k)-1}C}{\overline{f}(C)|_{t_{1,b}=0}} \delta(\overline{C})|_{t_{1,b}=0},$$

where $\widehat{\Gamma}$ is submanifold under the geometry constraints after attaching the BCFW bridge. We define $\widehat{C} \equiv \overline{C}|_{t_{1,b}=0}$ and transform minors of $C$ to those of $\widehat{C}$ by

$$(b\cdots) = (\widehat{b}\cdots) - \alpha(a\cdots), \tag{3.4}$$

where $(b\cdots)$ is any minor in $C$ that includes column $b$ and

$$\alpha = \frac{(b, a_2\cdots a_{k-m}, c_1\cdots c_m)}{(a, a_2\cdots a_{k-m}, c_1\cdots c_m)}. \tag{3.5}$$

Finally, we obtain the top form of the nonplanar diagram after attaching the bridge $(a, b)$:

$$\widehat{\mathcal{T}_n^k} = \oint_{\widehat{\Gamma}} \frac{d^{k\times(n-k)}\widehat{C}}{(b, a_2\cdots a_{k-m}, c_1\cdots c_m))\overline{f}(\widehat{C})}\delta(\widehat{C}). \tag{3.6}$$

For general nonplanar leading singularities we construct the top-form by attaching BCFW bridges step by step.

### A more general example of attaching a nonadjacent bridge

As an application, we take the nonplanar diagram in Fig. **??** as an example. According to the permutation of the planar diagrams before attaching the bridge $(1, 6)$,

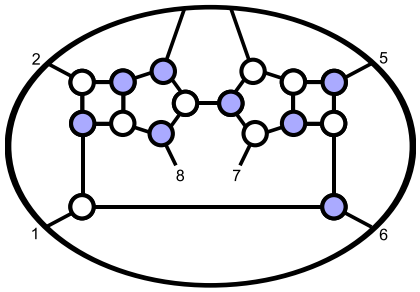


**Figure 8**. A nonplanar on-shell diagram of $\mathcal{A}_8^4$

linear relations of the diagram are $(4, 5, 6, 7)^2$ and $(8, 1, 2, 3)^3$. Attaching bridge $(1, 6)$ does not affect $(8, 1, 2, 3)^3$ while $(4, 5, 6, 7)^2$ alters. And

$$C = \begin{pmatrix} 1 & * & 0 & 0 & 0 & t_1 & t_3 & * \\ 0 & * & 1 & 0 & 0 & t_2 & t_4 & * \\ 0 & * & 0 & 1 & 0 & * & * & * \\ 0 & * & 0 & 0 & 1 & * & * & * \end{pmatrix}.$$

According to the discussion above (Eq. 3.3 – 3.6),

$$\begin{aligned}\widehat{\mathcal{T}_8^4} &= \int \frac{d\alpha}{\alpha} \oint_{\Gamma} \frac{d^{16}C}{(1234)(2345)(3456)(4567)(5678)(6781)(7812)(8123)}\delta(\overline{C}) \\ &= \int \frac{d\alpha}{\alpha} \oint_{\Gamma} \frac{dt_1}{t_1(4567)(5678)(6789)(7891)} \frac{d^{15}C}{(1234)(2345)(8123)}\delta(\overline{C}) \\ &= \oint_{\widehat{\Gamma}} \frac{d\alpha}{\alpha} \frac{d^{15}C}{(4567)(5678)(6789)(7891)|_{t_1=0}(1234)(2345)(8123)}\delta(\overline{C})|_{t_1=0} \\ &= \oint_{\widehat{\Gamma}} \frac{d^{16}\widehat{C}}{\alpha(4567)(5678)(6789)(7891)|_{t_1=0}(1234)(2345)(8123)}\delta(\widehat{C}),\end{aligned}$$

where $\alpha = \frac{(345\widehat{6})}{(1345)}$. Finally we obtain top form of $\mathcal{A}_8^4$:

$$\widehat{\mathcal{T}_8^4} = \oint_{\widehat{\Gamma}} \frac{d^{4\times 8}\widehat{C}}{vol(GL(4))} \frac{(1345)^2\delta(\widehat{C})}{(1234)(2345)(345\widehat{6})(45\widehat{61})(4537)(5784)(5\widehat{613})(\widehat{6781})(7812)(8123)}$$

Therefore, we can always construct the top-from of nonplanar diagrams by attaching adjacent and nonadjacent bridges on identity diagram step by step.

### The simplification of the MHV top-form

The MHV top-form can be further simplified. We can always transform any nonplanar MHV top-form into a summation of several top-forms. These generated top-forms share features that their numerators of the integrands equal 1 and the minors in $f(C)$ are of cyclic orders, which are exactly those of planar MHV top-forms. This yields a strong proof that any nonplanar MHV amplitude is a summation of several planar amplitudes.

To see this, let us consider the top-form of $\mathcal{A}_n^2$. Attaching a nonadjacent bridge $(a, b)$ to a planar diagram yields

$$\widehat{\mathcal{T}_n^2} = \int \frac{d\alpha}{\alpha} \oint_{\Gamma} \frac{d^{2\times n}C}{vol(GL(2))} \frac{\delta(C)}{(12)\cdots(b-1,b)(b,b+1)\cdots(n1)}$$

Without losing generality, we assume the pole at $(b-1, b) = 0$. Following the same procedure illustrated in Eq. 3.3 – 3.6, we obtain

$$\frac{1}{f(\widehat{C})} = \frac{(a,b-1)}{(12)\cdots(b-2,b-1)(b-1,\widehat{b})(a,\widehat{b})(b+1,b-1)(b+1,b+2)\cdots(n1)}$$

Since $a < b-1$, we define $a+m = b-1$ $(m \in \mathbb{Z}^+)$.

- If $m = 1$, the numerator is then $(b-2, b-1)$ and the integrand can be simplified to a term with its numerator equaling one and $f(C)$ of cyclic orders, i.e. a planar one.

- If $m > 1$ , we can multiply the numerator and denominator by $(a+1, \widehat{b})$:

$$\begin{aligned}\frac{1}{f(C)} &= \frac{(a,b-1)(a+1,\widehat{b})}{(12)\cdots(b-2,b-1)(b-1,\widehat{b})(a,\widehat{b})(b+1,b-1)(b+1,b+2)\cdots(n1)(a+1,\widehat{b})} \\ &= \frac{(a,a+1)(\widehat{b},b-1)+(a,\widehat{b})(a+1,b-1)}{(12)\cdots(b-2,b-1)(b-1,\widehat{b})(a,\widehat{b})(b+1,b-1)(b+1,b+2)\cdots(n1)(a+1,\widehat{b})} \\ &= \frac{1}{(12)\cdots(a-1,a)(a+1,a+2)\cdots(b-2,b-1)(a,\widehat{b})(b-1,b+1)(b+1)(b+2)\cdots(n1)(a+1,\widehat{b})}+ \\ &\quad \frac{(a+1,b-1)}{(12)\cdots(b-2,b-1)(b-1,\widehat{b})(a+1,\widehat{b})(b+1,b-1)(b+1,b+2)\cdots(n1)}.\end{aligned}$$

  The first term is already planar, while the second is not obvious.

  - If $m = 2$, the second term is planar.
  - If $m > 2$, we multiply the integrand by $(a+2, b), (a+3, b), \cdots, (a+m-1, b)$ one by one. For each step of multiplication, we utilize the Pluck relation to transform the nonplanar term into a summation of planar terms and a remaining term. The final term left after series of multiplication is

$$\frac{(a+m-1, b-1)}{(12)\cdots(b-2, b-1)(b-1, \widehat{b})(a+m-1, \widehat{b})(b+1, b-1)(b+1, b+2)\cdots(n1)}.$$

    Since $a + m = b - 1$, this term is also planar.

Following these steps, we can finally simplify the top-forms of all nonplanar MHV amplitudes into the sum of planar ones. One can easily verify that the simplification process from nonplanar one to planar term's summation is equivalent to applying KK relation to MHV amplitudes.

In this section, we construct the top-forms of the nonplanar on-shell graphs. The key step is attaching a nonadjacent BCFW bridge to a planar diagram. The cyclic order of $f(C)$ is then broken and we obtain a different integrand from the planar ones. Keep attaching bridges on the identity and we can arrive at the top-form of our target–the nonplanar leading singularity. We then break down the top-forms of the nonplanar MHV amplitudes into a summation of the planar top-forms. For the leading singularities of the one-loop amplitudes, this simplification is similar to the KK relation. For leading singularities of the general amplitudes, the relation between the top-form's simplification and the KK relation will be discussed in our future work.

## 4 Scattering amplitude: the *BCFW constructed form*

In the d*log* form and the top-form, we need to integrate the $\delta$ functions over the parameter space for the Grassmannian sub-manifold. This integration can be tedious as we need to solve all the $\alpha_I$'s at once–the array of constraint equations can be highly nonlinear. Recall that during the BCFW decompositions each parameter $\alpha_I$ is evaluated with respect to the external momenta upon removing one BCFW-bridge from the tree-level diagrams. Hence the $\delta$ functions can in fact be linearized for these resultant tree-level diagrams. For general leading singularities, the knowledge of BCFW recursion relations can still be used to linearize the $\delta$ functions to a convenient form—the BCFW constructed form.

A systematic way of constructing the BCFW constructed form follows the following steps.

- Choose a simplest partial graph from the leading singularity and *cut* it from the main diagram. Then we write down the marked permutations of the partial graph according to Section 2.

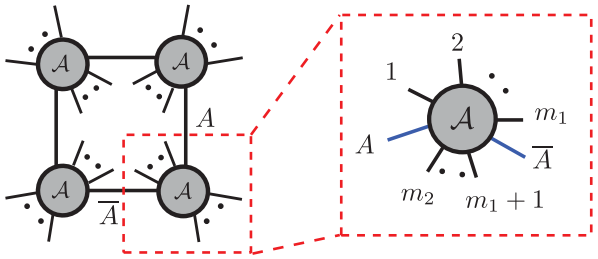


**Figure 9**. Choosing a partial graph

- According to the marked permutations of the partial diagram, we obtain the pole types generated by each step of BCFW-bridge decomposition. Then we choose a canonical order of BCFW-bridge decomposition chain based on the pole types. This step will be discussed in Section 4.1.

- During the process $U(1)$ decoupling relations may be applied to the partial graph according to Section 2. Upon the partial graph being disconnected we glue back the partial graph and obtain a planar diagram. Then we proceed decomposition under the canonical order until the diagram is decomposed to identity.

- Write down the linearized delta functions for the poles upon removing all BCFW-bridges in the canonical order. This step will be discussed in Section 4.2.

Finally we arrive at the expression of the leading singularity. For each decomposition chain

$$\begin{aligned}\mathcal{A}_n^k = &\int \frac{d\alpha_1}{\alpha_1} \wedge \cdots \wedge \frac{d\alpha_{2n-4}}{\alpha_{2n-4}} \prod_{h=1}^{n_p} \delta(\hat{p}_h^2)\delta^{2\times 2}(\lambda\cdot\tilde{\lambda})\delta^{2\times 4}(\lambda\cdot\tilde{\eta}) \\ &\times \prod_{i=1}^{n_w} \delta\left([i\ I_w]^2[i\ i-1]\alpha_i - \frac{1}{\overline{\mathcal{A}}_{W_i}}\right)[i-1\ i]^4 \\ &\times \prod_{j=1}^{n_b} \delta\left(\langle j\ I_b\rangle^2\langle j\ j+1\rangle\alpha_j - \frac{1}{\overline{\mathcal{A}}_{B_j}}\right)\langle I_b\ j+1\rangle^4\delta^{1\times 4}\left(\tilde{\eta}_j + \frac{\langle I\ j\rangle}{\langle I\ j+1\rangle}\tilde{\eta}_{j+1}\right) \\ &\times \delta(\alpha - 1) \end{aligned} \tag{4.1}$$

where $\overline{\mathcal{A}}_{W_i} = \frac{1}{[i-1\ i][i\ I][I\ i-1]}$ and $\overline{\mathcal{A}}_{B_i} = \frac{1}{\langle j\ j+1\rangle\langle j+1\ I\rangle\langle I\ j\rangle}$. There are two types of poles.

- A $\delta(\hat{p}_h^2)$ indicates the local pole after removing a BCFW-bridge.

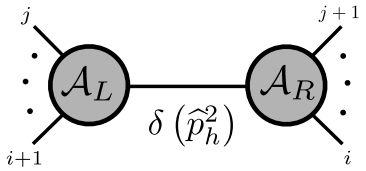


**Figure 10**. A local pole as a factorization channel

- A $\delta(c\alpha - 1/\mathcal{A})$ indicates one type of non-local poles. It will form a three point amplitude, or an identity, upon integrating over $\frac{d\alpha}{\alpha}$. It emerges upon removing the BW-bridges $\mathcal{B}(i-1, i, \alpha_i)$ or $\mathcal{B}(j, j+1, \alpha_j)$ on white or black vertices with a pair of external legs $\{i-1, i\}$ or $\{j, j+1\}$. In general cases, non-local poles emerge upon the diagrams being disconnected through splitting into two subgraphs after a bridge removal.

**Figure 11**. two types of non-local poles as white or black vertices

### 4.1 Marked permutations, pole types and the canonical order

The marked permutations of the unglued graphs determine the BCFW decomposition chain. The chain is, however, not unique. In the BCFW constructed form, the BCFW-bridge decompositions are performed in a canonical order. In this subsection, first we utilize the marked permutation to determine the two types of poles generated by each step of bridge removal. To achieve this goal, we introduce the Exterior Permutations Number table (the EPN table). Next we introduce the canonical order to choose the best decomposition chain for computing the amplitude.

#### The EPN table

A useful tool to find the constraints on $\alpha$ variables and pole types of the amplitude from the permutations is using the EPN table. Consider a group of external line $g_{ij} = \{i, i+1, \ldots, j-1, j\}$. The exterior permutations number $\mathcal{P}(g_{ij})$ defined on this group $g_{ij}$ is the number of legs $w$ in the group whose $\sigma(w)$ is not in the group. Table 4.1 is a general EPN table for m points graph.

**Table 2**. The EPN table

| | | | | | |
|---|---|---|---|---|---|
| $\mathcal{P}(\{1\})$ | $\mathcal{P}(\{2\})$ | $\mathcal{P}(\{3\})$ | $\cdots$ | $\mathcal{P}(\{m-2\})$ | $\mathcal{P}(\{m-1\})$ |
| | $\mathcal{P}(\{1,2\})$ | $\mathcal{P}(\{2,3\})$ | $\cdots$ | $\mathcal{P}(\{m-3,m-2\})$ | $\mathcal{P}(\{m-2,m-1\})$ |
| | | $\mathcal{P}(\{1,2,3\})$ | $\cdots$ | $\mathcal{P}(\{m-4,m-3,m-2\})$ | $\mathcal{P}(\{m-3,m-2,m-1\})$ |
| | | | $\ddots$ | $\vdots$ | $\vdots$ |
| | | | | $\mathcal{P}(\{1,\ldots,m-2\})$ | $\mathcal{P}(\{2,\ldots,m-1\})$ |
| | | | | | $\mathcal{P}(\{1,\ldots,m-1\})$ |

Each time we perform a BCFW-bridge decomposition, the EPN table changes accordingly: Upon removing the bridge $(w\ w+1)$, only the groups containing one element of $\{w, w+1\}$ and one of $\{\sigma(w), \sigma(w+1)\}$ will have their exterior permutations' quantities decrease by 1. We keep track of all the modifications in the EPN table during the chain of decompositions and pay special attention to the pole-contributing ones $2 \to 1$ and $1 \to 0$ in the process. For a certain set of external lines $\{i \ldots j\}$ of an on-shell digarm, after removing one bridge the $\mathcal{P}(g_{ij})$ modification

- $2 \to 1$ represents separating the diagram into two subgraphs–one of which is the subgraph labeled by $\{i \ldots j\}$–connected by one internal line. The on-shell internal line is then a local pole as shown in Fig. 10, giving constraint $(p_i + p_{i+1} + \ldots + p_j)^2 = 0$.

- $1 \to 0$ represents a subgraph labeled by $\{i \dots j\}$ being entirely disconnected from the remaining diagram. It then produces a non-local pole in the amplitude, giving constraint $p_i + p_{i+1} + \ldots + p_j = 0$. As an example, see Fig. 11.

To better illustrate our approach, we shall see how the EPN table method works in $\mathcal{A}_6^3$ with the permutation

$$\sigma = \begin{pmatrix} 1\ 2\ 3\ 4\ 5\ 6 \\ \downarrow\ \downarrow\ \downarrow\ \downarrow\ \downarrow\ \downarrow \\ 4\ 6\ 5\ 7\ 8\ 9 \end{pmatrix}.$$

As for $(3\ 4\ 5) \to (5\ 7\ 8)$, for instance, external lines $7, 8$ do not belong to group $(3\ 4\ 5)$ while 5 is at the same time $\sigma(3)$ and one element of the group, thus $\mathcal{P}(\{3,4,5\}) = 2$. Keep numerating until the complete EPN table is obtained. If we remove the $(1,2)$ bridge, the new permutation reads $(6,4,5,7,8,9)$,

$$\begin{array}{ccccc} 1 & 1 & 1 & 1 & 1 \\ & 2 & 2 & 2 & 2 \\ & & 3 & 3 & 2 \\ & & & 2 & 2 \\ & & & & 1 \end{array} \quad \Longrightarrow \quad \begin{array}{ccccc} 1 & 1 & 1 & 1 & 1 \\ & 2 & 2 & 2 & 2 \\ & & 3 & 2 & 2 \\ & & & 2 & 1 \\ & & & & 1 \end{array}.$$

The groups containing one line from $\{1,2\}$ and one line from$\{3,4\}$ have their EPN values altered in the process. In this example, the modification of $\mathcal{P}(\{2,3,4\})$ is $3 \to 2$ and that of $\mathcal{P}(\{2,3,4,5\})$ is $2 \to 1$. Recall what we are interested in are those with modifications $2 \to 1$ and $1 \to 0$. The former case then yields the constraint imposed on $\alpha$ in this example, which is $(\hat{p}_2 + p_3 + p_4 + p_5)^2 = 0$. The remaining deformation variables can be obtained in the same way.

The modifications in the EPN table label two types of constraints and poles. According to these two pole types, we can define a canonical order of BCFW-bridge decompositions. *Note* that if we are decomposing a partial graph utilizing the marked permutation, the "pole" and the constraint we obtain by the EPN modifications may not be the correct one. We shall discuss this case in next paragraph.

### The canonical order

The canonical order consists of two rules:

- Bridge decompositions mustn't cross any already-obtained local pole.
- Disconnected graph except for identity is forbidden.

As stated in the introduction of this section, we first perform bridge decompositions on the partial graph utilizing the marked permutation. Since the partial graph needs to be glued back, the "poles" obtained by the EPN table may not be the correct ones. Each time we obtain a "pole" in a partial graph, we should verify if it is a correct one by looking at the whole diagram. In order to illustrate the two rules of the canonical order, we list all possible conditions one may encounter during bridge removals. We categorize all situations according to $\mathcal{P}$ and the pole types.

**$2 \to 1$ as a local pole**

For the planar diagram after gluing back the partial graph, bridge decomposing and obtaining poles by the EPN always give the correct answer. Thus we write down the delta functions in the amplitude according to Section 4.2.

Next we consider the partial graph with two gluing lines $A$ and $\bar{A}$. Consider the group $g_{ij}$ that undergoes the $\mathcal{P}(g_{ij}) : 2 \to 1$ modification. If both or neither of $\{A, \bar{A}\}$ are included in $g_{ij}$ then the "pole" is an 1-line reducible channel (1LR). Otherwise it is an 1-line irreducible channel (1LI).

- For 1LR shown in Fig. 12, one can verify that the 1LR always gives the correct pole in the partial graph. We write down the delta function in the amplitude according to Section 4.2. According to the first rule of the canonical order, once this local pole is obtained we cannot perform BCFW decompositions across it any more. Upon removing the bridge the whole diagram factorizes into $\mathcal{A}_L(p_A, p_{\bar{A}}) \cdot \mathcal{A}_R$. We shall first fully decompose $\mathcal{A}_R$ and then go back to $\mathcal{A}_L(p_A, p_{\bar{A}})$.

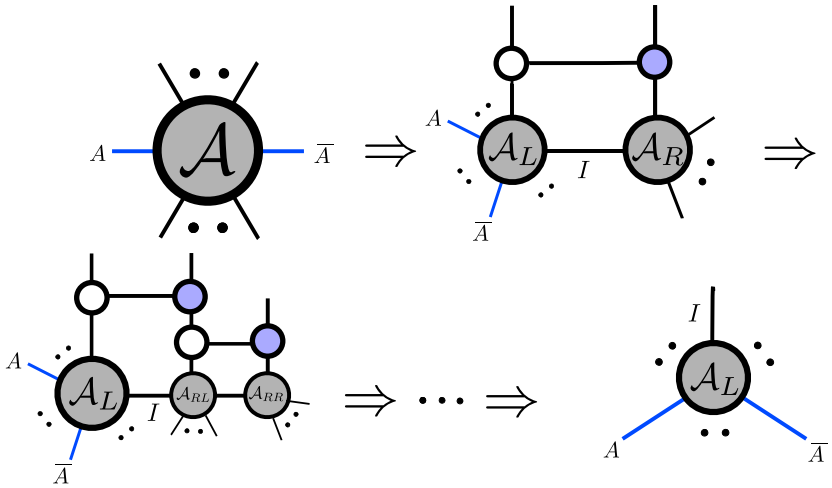


**Figure 12**. 1-line reducible channel

- For 1LI shown in Fig. 13, the "pole" we obtain from EPN is not correct, since after gluing back the partial graph the "pole" no longer exists. Since the "pole" is not a correct local pole, the first rule of the canonical order does not apply. Thus we *do not* write down the delta function in the amplitude but save it until we glue back the partial graph. After a bridge removal, the partial graph falls into $\mathcal{A}_L(p_A)$ and $\mathcal{A}_R(p_{\bar{A}})$. Then we choose the simpler diagram of $\mathcal{A}_L(p_A)$ and $\mathcal{A}_R(p_{\bar{A}})$ and *redefine* it as the new partial graph. Repeating the procedures above, the size of the partial graph drops rapidly as shown in Fig. 13(a). The advantage of this strategy is that it takes fewer steps to unfold the loop. The partial graph will finally arrive at a planar box or a nonplanar box. If the box is nonplanar as shown in Fig. 13(c) we shall apply $U(1)$ decoupling relation to twist the box and arrive at Fig. 13(b). To unfold the loop in the planar box case we remove a WB- and a BW- bridge. After the loop is unfolded we glue back the partial graph. Then we refer to the EPN table of the whole diagram and write down all the delta functions of $\mathcal{P}(g_{ij}) = 1$ according to Eq. 4.3.

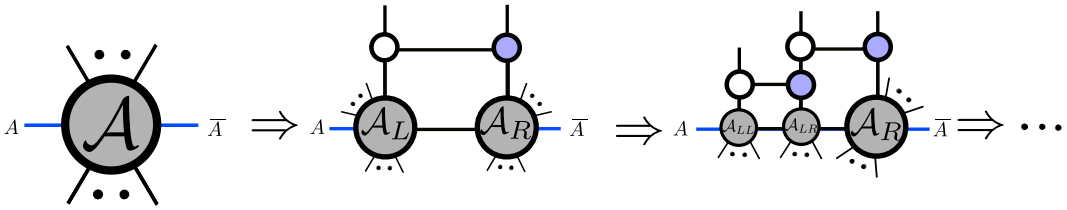


(a) the decomposition chain of 1LI

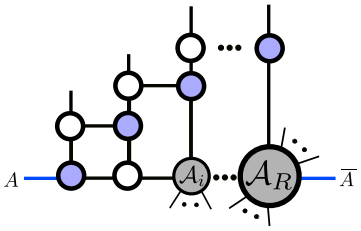


(b) a planar box as the final partial graph

or

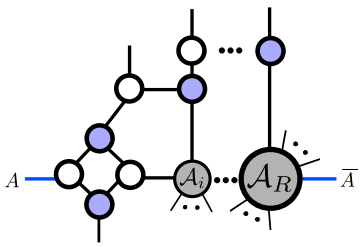


(c) a nonplanar box as the final partial graph

**Figure 13**. 1-line irreducible channel

**$1 \to 0$ as a non-local pole**

- If a white or a black three-point vertex becomes the identity, the pole is allowed by the canonical order. Then we write down the delta function in the amplitude according to Section 4.2.

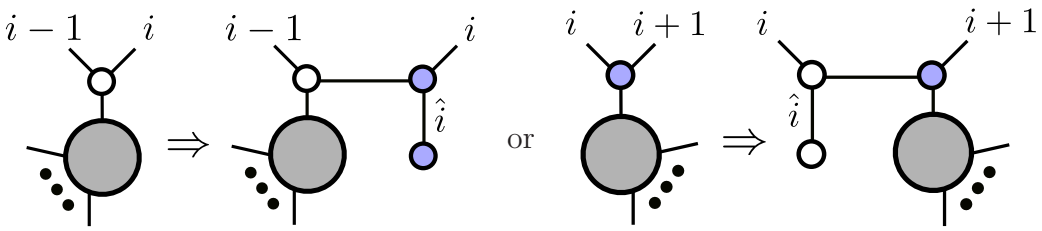


**Figure 14**. A non-local pole as an identity

- If there comes no identity, the result is a disconnected graph. The disconnected graph is forbidden by the canonical order. We should try another bridge.

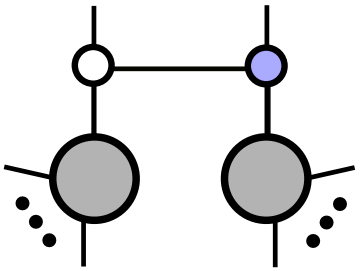

**Figure 15**. A non-local pole as a disconnected graph.

For now we have discussed the canonical order of BCFW-bridge decomposition. First we label different bridge decompositions according to their EPN modifications. For each types of EPN modification, we obtain the corresponding pole types. Then we define the canonical order and select an explicit BCFW chain accordingly. With the canonical order, we can decompose the leading singularities in an extremely efficient manner. The only missing piece is the calculation result of the delta function of each pole, which we shall present in the next subsection.

### 4.2 Amplitude recursion relation under the canonical order

The BCFW-bridge will import an integration over $\frac{d\alpha}{\alpha}$ into the amplitude which shall be fixed by the local poles and non-local poles. These two poles arise when some $g_{ij} \to 1$ and $g'_{i'j'} \to 0$ appear in EPN table. Inspired by BCFW recursion relation in the tree-level diagram [1–4] , we can write down the poles in the leading singularities' amplitudes in terms of on-shell propagators and three-vertexes. In this section, we calculate the delta functions of each type of poles and the supermomentum factors of the amplitudes.

**Recursion relation of the local pole**

When $g_{ij} \to 1$, the amplitude $\mathcal{A}$ factorizes into $\mathcal{A}_L$ and $\mathcal{A}_R$:

$$\begin{aligned}\mathcal{A} = &\int \frac{d\alpha}{\alpha} \int \frac{d^2\lambda_I d^2\tilde{\lambda}_I d^4\eta_I}{vol(GL(1))} \mathcal{A}_L(p_I(\alpha), \eta_I) \delta^{2\times 2}\left(\sum p_{L,j} - p_I(\alpha)\right) \\ &\times \mathcal{A}_R(p_I(\alpha), \eta_I) \delta^{2\times 2}\left(\sum p_{R,j} + p_I(\alpha)\right) \\ = &\int \frac{d\alpha}{\alpha} \int d^4p_I d^4\eta_I \ \delta\left(p_I(\alpha)^2\right) \mathcal{A}_L(p_I(\alpha), \eta_I) \mathcal{A}_R(p_I(\alpha), \eta_I) \\ &\times \delta^{2\times 2}\left(\sum p_{L,j} - p_I(\alpha)\right) \delta^{2\times 2}\left(\sum p_{R,j} + p_I(\alpha)\right) \\ = &\int \frac{d\alpha}{\alpha} \int d^4\eta_I \ \delta\left(p_I(\alpha)^2\right) \mathcal{A}_L(p_I(\alpha), \eta_I) \mathcal{A}_R(p_I(\alpha), \eta_I) \\ &\times \delta^{2\times 2}\left(\sum p_{L,j} + \sum p_{R,j}\right). \end{aligned} \tag{4.2}$$

Thus each time we obtain a local pole we write down a delta function $\delta\left(p_I(\alpha)^2\right)$ and keep in mind that the supermomentum integration is left to be evaluated later.

One-bridge-one-pole correspondence is not always true. Recall the 1LI case in Section 4.1. After removing the bridge we do not write down the delta function immediately. Upon gluing back the partial graph all local poles we missed before will jump out at once. Similar to the discussion above, we arrive at a set of several coupled equations of variables $\alpha_{h_1}\alpha_{h_2}\cdots\alpha_{h_{M-1}}$ and the amplitude has the form:

$$\mathcal{A} = \int \prod_{i=1}^{M-1} d^4\eta_{I_i} \int \bigwedge_{i=1}^{M-1} \frac{d\alpha_{h_i}}{\alpha_{h_i}} \mathcal{A}_1 \delta\left(\hat{p}_{I_1}^2\right) \mathcal{A}_2 \delta\left(\hat{p}_{I_2}^2\right) \cdots \mathcal{A}_{M-1} \delta\left(\hat{p}_{I_{M-1}}^2\right) \mathcal{A}_M \delta^{2\times 2}\left(\sum p_e\right) \tag{4.3}$$

where the $p_I$'s are functions of $\alpha_i$.

In the local pole cases, most of the delta functions are linear.

$$\begin{aligned} &\int \frac{d\alpha}{\alpha} \delta\left[\left(p_{L,1} + p_{L,2} + \ldots + p_{L,i} - \alpha\lambda_a\tilde{\lambda}_b\right)^2\right] \\ = &\int \frac{d\alpha}{\alpha} \delta\left(s_{1,2,\ldots,i} - \alpha\langle a|p_{1,\ldots,i}|b]\right). \\ = &\frac{1}{s_{1,2,\ldots,i}}. \end{aligned} \tag{4.4}$$

The only exception is the final three $\alpha$'s fixed by delta functions on line $I_a$, $I_b$ and $I_c$ in Fig. 16. These three delta functions are usually quadratic and have two solutions.

The momentum $p_A$ of the loop line A is determined by the three delta functions. We can substitute $p_A$ into other delta functions. As a result, all other delta functions on $\alpha$'s will become linear.

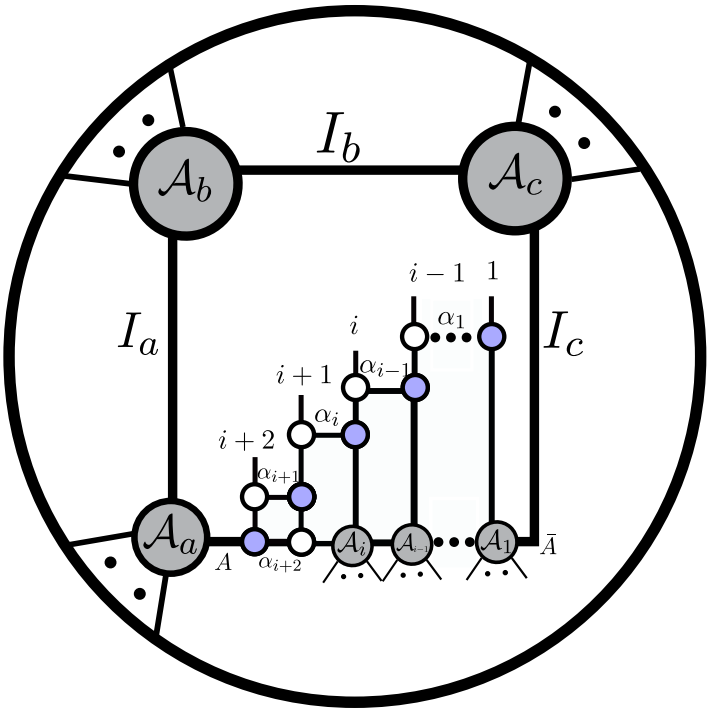


**Figure 16**. The BCFW-bridge to open the loop of the diagram.

### Recursion relations of the non-local pole

In the canonical order, the only allowed non-local poles are black and white three-point vertexes.

- After a BW-bridge on a white vertex is removed, the amplitudes transform as

$$\begin{aligned}
&\begin{array}{l} i \\ \\ i-1 \end{array}\!\!\!\diagup\!\!\!

- After a BW-bridge on a black vertex is removed, the amplitudes transform as

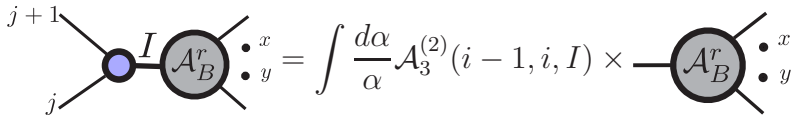


$$= \int \frac{d\alpha}{\alpha} \mathcal{A}_3^{(2)}(i-1,i,I) \times$$

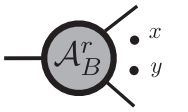


$$= \int \frac{d\alpha}{\alpha} \delta\left(\langle j\ I\rangle^2 \langle j\ j+1\rangle \alpha - \frac{1}{\overline{\mathcal{A}}_3^{(2)}(i-1,i,I)}\right) \times$$

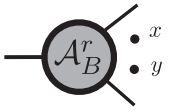


$$= \int \frac{d\alpha}{\alpha} \delta\left(\langle j\ I\rangle^2 \langle j\ j+1\rangle \alpha - \langle i-1\ i\rangle \langle i\ I\rangle \langle I\ i-1\rangle\right) \times$$

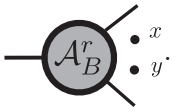


. (4.6)

- Decompositions of two external lines is trivial.

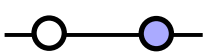

$$= \int \frac{d\alpha}{\alpha} \delta(\alpha - 1) = 1. \tag{4.7}$$

**supermomentum factors**

Until now we have not mentioned the supersymmetry part. Since a BCFW-bridge does not contribute supermomentum factors, these factors originate merely from super-parameter integration over internal lines between each two vertices.

According to Eq. 4.2, a local pole line contributes an integration over the single channel line $\int d^4\eta_I$. According to the definition in [43], a white vertex $\mathcal{A}_3^w(12I)$ contributes

$$\delta^{1\times 4}\left([2I]\tilde{\eta}_1 + [I1]\tilde{\eta}_2 + [12]\tilde{\eta}_I\right),$$

and a black vertex $\mathcal{A}_3^b(12I)$ contributes

$$\delta^{2\times 4}\left(\lambda_1\tilde{\eta}_1 + \lambda_2\tilde{\eta}_2 + \lambda_I\tilde{\eta}_I\right).$$

The integration $\int d^4\eta_I$ could be done upon the evaluation of a white or black vertex. The factors are as follows:

$$\int d^4\tilde{\eta}_I \delta^{1\times 4}\left([2I]\tilde{\eta}_1 + [I1]\tilde{\eta}_2 + [12]\tilde{\eta}_I\right) = [12]^4 \tag{4.8}$$

and

$$\begin{aligned}
&\int d^4\tilde{\eta}_I \delta^{2\times 4}\left(\lambda_1\tilde{\eta}_1+\lambda_2\tilde{\eta}_2+\lambda_I\tilde{\eta}_I\right)\\
&=\int d^4\tilde{\eta}_I\left(\frac{1}{\langle 12\rangle}\right)^4\delta^{1\times 4}\left(\langle 21\rangle\tilde{\eta}_1+\langle I1\rangle\tilde{\eta}_I\right)\delta^{1\times 4}\left(\langle 12\rangle\tilde{\eta}_2+\langle I2\rangle\tilde{\eta}_I\right)\\
&=\left(\frac{\langle I2\rangle}{\langle 12\rangle}\right)^4\delta^{1\times 4}\left(\langle 21\rangle\tilde{\eta}_1-\langle I1\rangle\frac{\langle 12\rangle}{\langle I2\rangle}\tilde{\eta}_2\right)\\
&=\langle I2\rangle^4\delta^{1\times 4}\left(\tilde{\eta}_1+\frac{\langle I1\rangle}{\langle I2\rangle}\tilde{\eta}_2\right). \qquad (4.9)
\end{aligned}$$

Now, with the final missing piece retrieved, we have the whole story of the BCFW constructed forms of one-loop leading singularities. We can obtain the explicit amplitude of an one-loop leading singularitiy—be it planar or nonplanar— almost as conveniently as we do for tree-level diagrams. In order to display the superiority of our methodology, we provide two examples as follows:

### 4.3 Examples

In this subsection, we will work out two examples in details. Recall that according to permutations, nonplanar leading singularities can be categorized into three groups. Our calculation, however, will not lose generality for the fact that after twisting one planar leg or twisting a nonplanar box, either case will fall into External line Pairs. Thus we calculate Black-White Chain $\mathcal{A}_6^3$ and Box Chain $\mathcal{A}_8^4$.

**Black-White Chain $\mathcal{A}_6^3$**

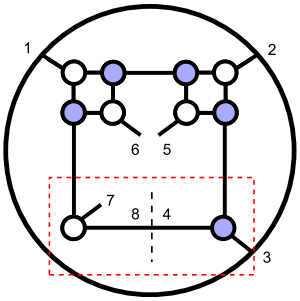


**Figure 17**. Black-White Chain $\mathcal{A}_6^3$

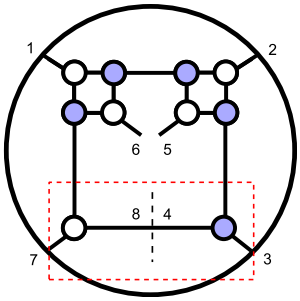


**Figure 18**. Black-White Chain $\mathcal{A}_6^3$ after twisting a leg

As an example of Black-white Chain, we calculate $\mathcal{A}_6^3$. We extract the partial graph as shown in Fig. 17. The partial graph includes external legs 3 and 7 as well as two legs 4 and 8.

Obviously, the partial graph is already a "skeleton diagram", specifically a black-white chain, which requires twisting the leg into planar one and multiply by $(-1)$. The partial graph the transforms into the $(7,3)$ Go on to remove this White-Black bridge,

$$\left\{\begin{array}{c}\lambda_7 \to \lambda_{\widehat{7}} = \lambda_7 \\ \widetilde{\lambda}_7 \to \widetilde{\lambda}_{\widehat{7}} = \widetilde{\lambda}_7 - \alpha\widetilde{\lambda}_3\end{array}\right\} \quad \text{and} \quad \left\{\begin{array}{c}\lambda_3 \to \lambda_{\widehat{3}} = \lambda_3 + \alpha\lambda_7 \\ \widetilde{\lambda}_3 \to \widetilde{\lambda}_{\widehat{3}} = \widetilde{\lambda}_3\end{array}\right\}, \tag{4.10}$$

and the loop is unfolded. To obtain the corresponding constraint we should refer to the EPN table of the whole graph

| 1 | 2 | $\widehat{3}$ | 5 | 6 |
|---|---|---|---|---|
| 1 | 1 | 1 | 1 | 1 |
| | 2 | 2 | 2 | 2 |
| | | 3 | 1 | 3 |
| | | | 2 | 2 |
| | | | | 1 |

.

As $\mathcal{P}(\{2,\widehat{3},5\})$ becomes 1, we obtain a local pole:

$$p_{I_1} = (p_2 + p_{\widehat{3}} + p_5)^2 = 0, \tag{4.11}$$

$$\alpha = \frac{p_{235}^2}{\langle 7|p_{235}|3]} \qquad p_{I_2} = \frac{p_{235}|3] \otimes p_{235}|7\rangle}{\langle 7|p_{235}|3]}. \tag{4.12}$$

We proceed to seek all remaining propagators and the graph is decomposed into bare three-point amplitudes, i.e.

$$\mathcal{A}_6^3 = \int \frac{d\alpha_1}{\alpha_1} \wedge \frac{d\alpha_2}{\alpha_2} \wedge \frac{d\alpha_3}{\alpha_3} \delta(\hat{p}^2_{2\widehat{35}})\delta(\hat{p}^2_{\widehat{35}})\delta(\hat{p}^2_{\widehat{2356}}) \times$$

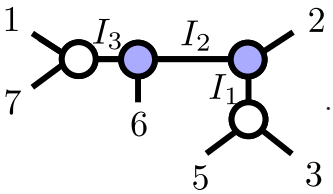


. (4.13)

Then we further evaluate the non-local poles starting from one end of the chain. Each time when we send an external line to identity, a deformation variable will be extracted from the amplitude and the corresponding delta function is shown in Eq. 4.5 and 4.6.

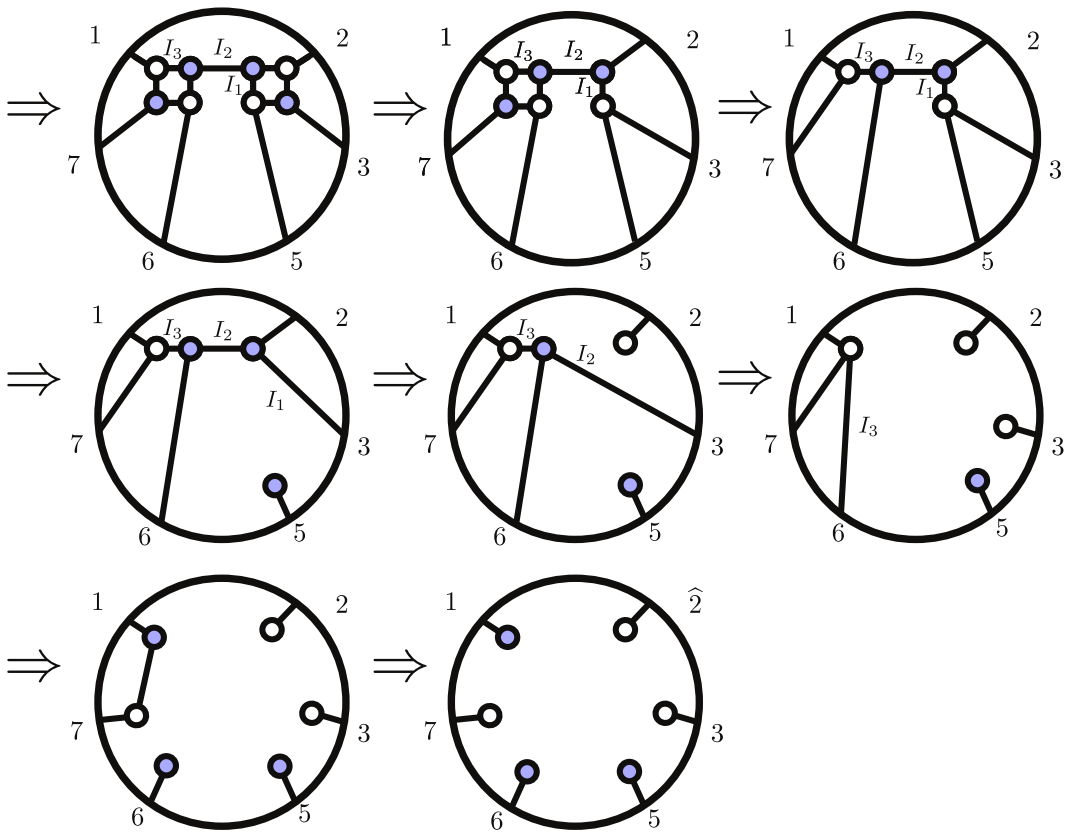


**Figure 19**. The BCFW decomposition chain of $A_6^3$

We should also consider supermomentum factors in Eq. 4.8 and 4.9. Finally we can write down the amplitude in form of Eq. 4.1 as follows:

$$\begin{aligned}
\mathcal{A}_6^3 = & \int \frac{d\alpha_1}{\alpha_1} \wedge \cdots \wedge \frac{d\alpha_8}{\alpha_8} \delta(\hat{p}^2_{2\widehat{3}5}) \delta(\hat{p}^2_{\widehat{2}\widehat{3}5}) \delta(\hat{p}^2_{2\widehat{2}\widehat{3}5\widehat{6}}) \delta^{2\times 2}(\lambda \cdot \tilde{\lambda}) \delta^{2\times 4}(\lambda \cdot \tilde{\eta}) \\
& \times \delta\left( \frac{[5I_1]^2[53]\alpha_4 - 1}{\mathcal{A}^W_{35I_1}} \right) [3,5]^4 \\
& \times \delta\left( \langle 2I_2\rangle^2 \langle 2I_1\rangle \alpha_5 - \frac{1}{\mathcal{A}^B_{2I_1I_2}} \right) \langle I_2 I_1\rangle^4 \delta^{1\times 4}\left( \tilde{\eta}_2 + \frac{\langle I_2, 2\rangle}{\langle I_2 I_1\rangle} \tilde{\eta}_{I_1} \right) \\
& \times \delta\left( \langle I_2 I_3\rangle^2 \langle I_2 6\rangle \alpha_6 - \frac{1}{\mathcal{A}^B_{I_26I_3}} \right) \langle I_3 6\rangle^4 \delta^{1\times 4}\left( \tilde{\eta}_{I_2} + \frac{\langle I_3, I_2\rangle}{\langle I_3 6\rangle} \tilde{\eta}_6 \right) \\
& \times \delta\left( \frac{[1I_3]^2[17]\alpha_7 - 1}{\mathcal{A}^W_{71I_3}} \right) \delta^{1\times 4}\left( [6, I_3]\tilde{\eta}_{I_2} + [I_3, I_2]\tilde{\eta}_6 + [I_2, 6]\tilde{\eta}_{I_3} \right) \\
& \times \delta\left( \alpha_8 - 1 \right).
\end{aligned} \tag{4.14}$$

A fast approach to work out the fat expression above is to recombine the three-point

amplitudes together to form larger amplitudes. It is easy to verify that the combination of the white point and black point in the left is $\mathcal{A}(6,\widehat{7},1,I_2)$ and $\mathcal{A}(I_2,2,\widehat{3},5)$ in the right. The two $\mathcal{A}_4^2$ can be further combined. Using a small technique to deal with $\widehat{\lambda}_3$,

$$\begin{aligned}|\widehat{3}\rangle &= |3\rangle + \frac{p_{235}^2}{\langle 7|p_{235}|3]}|7\rangle \\ &= \frac{1}{\langle 7|p_{235}|3]}(|3\rangle\langle 7|p_{235}|3] - |7\rangle\langle 3|p_{235}|3] + p_{25}^2|7\rangle) \\ &= \frac{1}{\langle 7|p_{235}|3]}(\langle 73\rangle p_{235}|3] + p_{25}^2|7\rangle). \end{aligned} \tag{4.15}$$

The final amplitude then yields

$$\begin{aligned}\mathcal{A} &= \int d^4\widetilde{\eta_{I_2}}\mathcal{A}(6,\widehat{7},1,I_2)\frac{1}{s_{235}}\mathcal{A}(I_2,2,\widehat{3},5) \\ &= \frac{\langle 7|p_{25}|3]^2[35]^3}{\langle 67\rangle\langle 71\rangle\langle 1|p_{25}|3]\langle 6|p_{25}|3]s_{235}\langle 7|p_{23}|5]\langle 7|p_{35}|2][23]} \\ &\quad\times\delta^{1\times 4}(\widetilde{\eta}_2 + \frac{\langle 7|(p_3\circ p_{25}+p_{25}^2)\circ p_{25}|3]}{\langle 7|p_{25}|3][35]\langle 52\rangle}\widetilde{\eta}_3 + \frac{[23]}{[35]}\widetilde{\eta}_5) \\ &\quad\times\delta^{2\times 4}(\lambda_1\widetilde{\eta}_1 + \lambda_2\widetilde{\eta}_2 + \lambda_3\widetilde{\eta}_3 + \lambda_4\widetilde{\eta}_4 + \lambda_5\widetilde{\eta}_5 + \lambda_6\widetilde{\eta}_6). \end{aligned} \tag{4.16}$$

Remember this is the amplitude of the twisted diagram, i.e. a Black-White Pair case. And the corresponding Black-White Chain case's amplitude should be the opposite.

**Box Chain $\mathcal{A}_8^4$**

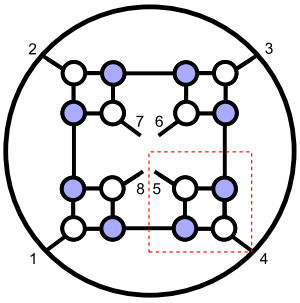


**Figure 20**. Box Chain $\mathcal{A}_8^4$

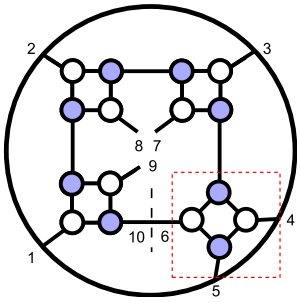


**Figure 21**. Box Chain $\mathcal{A}_8^4$ with one box twisted

Box Chain $\mathcal{A}_8^4$ is a symmetrical diagram with four nonplanar boxes. In this diagram, we should choose any one nonplanar box as the partial graph. Since we cannot remove any bridge on a nonplanar box, we need to apply $U(1)$ decoupling relation to

twist at least one box. The corresponding scattering amplitude is the sum of two diagrams'. Following the canonical order, we can first remove a White-Black bridge $(4,5)$ on the twisted partial graph, which does not produce an obvious propagator we usually encounter in tree level amplitudes. In the meantime, the loop still exists. We now go on to remove a Black-White bridge $(5,4)$. The diagram is then purely planar now for the loop has been unfolded. The diagram left is nothing but three boxes connecting together. Multiply them and integrate over two connecting lines, we can then arrive at the final amplitude of the Fig. 21. The first two steps of BCFW-bridge decompositions enable line 4 and 5 deformed by a scale,

$$\left\{\begin{array}{l}\lambda_{\widehat{4}}=\lambda_4+\alpha_2(\lambda_5+\alpha_1\lambda_4)\\ \widetilde{\lambda}_{\widehat{4}}=\widetilde{\lambda}_4-\alpha_1\widetilde{\lambda}_5\end{array}\right\}\quad\text{and}\quad\left\{\begin{array}{l}\lambda_{\widehat{\widehat{5}}}=\lambda_5+\alpha_1\lambda_4\\ \widetilde{\lambda}_{\widehat{\widehat{5}}}=\widetilde{\lambda}_5-\alpha_2(\widetilde{\lambda}_4-\alpha_1\widetilde{\lambda}_5)\end{array}\right\}. \tag{4.17}$$

$\alpha_1$ and $\alpha_2$ can be determined by sending internal momenta $I_1$ and $I_2$ on-shell, which yields,

$$\left\{\begin{array}{l}(p_{\widehat{4}}+p_3+p_7)^2=0\\ (p_{\widehat{\widehat{5}}}+p_1+p_9)^2=0\end{array}\right. . \tag{4.18}$$

If we replace $p_{\widehat{\widehat{5}}}$ by $p_4+p_5-p_{\widehat{4}}$ and denote $\alpha_2$ by $\alpha_1$,

$$\alpha_2=\frac{(p_{\hat{5}}+p_3+p_7)^2}{\langle\hat{5}|p_{3\hat{5}7}|\hat{4}]}=-\frac{(p_{\hat{5}}-p_1-p_4-p_5-p_9)^2}{\langle\hat{5}|p_{1459}|\hat{4}]} \tag{4.19}$$

where $p_{ij\cdots k}=p_i+p_j+\cdots+p_k$, $|\hat{5}\rangle=|5\rangle+\alpha_1|4\rangle$ and $|\hat{4}]=|4]-\alpha_1|5]$. By eliminating $\alpha_2$, we can obtain $\alpha_1$ by solving the equation

$$\frac{s_{3457}-\langle4|p_{37}|5]\alpha_1}{\langle5|p_{37}|4]-(p_3p_4+p_4p_7)\alpha_1-\langle4|p_{37}|5]\alpha_1^2}=\frac{-s_{149}-\langle4|p_{19}|5]\alpha_1}{\langle5|p_{19}|4]-(p_1p_4+p_4p_9)\alpha_1-\langle4|p_{19}|5]\alpha_1^2}. \tag{4.20}$$

This is a quadratic equation of $\alpha_1$, which gives two solutions, namely $\alpha_{1+}$ and $\alpha_{1-}$. With values of $\alpha$ clear by now, we can immediately work out the other two internal line momenta using

$$I_1=\frac{p_{1\hat{5}9}\mid\widehat{4}]\otimes p_{1\hat{5}9}\mid\widehat{\hat{5}}\rangle}{\langle\widehat{5}\mid p_{1\hat{5}9}\mid\widehat{4}]}\qquad I_2=\frac{p_{12\hat{5}89}|\widehat{4}]\otimes p_{12\hat{5}89}|\widehat{\hat{5}}\rangle}{\langle\widehat{5}|p_{12\hat{5}89}|\widehat{4}]}. \tag{4.21}$$

We now construct the full amplitude for twisted box chain $\mathcal{A}_8^4$, which is

$$\begin{aligned}\mathcal{A}_8^4=&\int\frac{d^2\lambda_{I_1}d^2\widetilde{\lambda}_{I_1}}{vol(GL(1))}\frac{d^2\lambda_{I_2}d^2\widetilde{\lambda}_{I_2}}{vol(GL(1))}\frac{d\alpha_1}{\alpha_1}\frac{d\alpha_2}{\alpha_2}\delta(I_1+p_1+p_9+\widehat{\widehat{5}})\\ &\times\delta(I_1+I_2+p_2+p_8)\mathcal{A}_4^2\mathcal{A}_4^2\mathcal{A}_4^2,\end{aligned} \tag{4.22}$$

where $\mathcal{A}_4^2\mathcal{A}_4^2\mathcal{A}_4^2$ represents integration

$$
\begin{aligned}
&\int d^4\widetilde{\eta}_{I_1} d^4\widetilde{\eta}_{I_2} \mathcal{A}(9,\hat{\hat{5}},1,I_1)\mathcal{A}(I_1,2,I_2,8)\mathcal{A}(I_2,3,\hat{\hat{4}},7) \\
=& \frac{[\hat{4}|p_{1\hat{5}9}|1\rangle^3}{\langle 9\hat{5}\rangle\langle 1\hat{5}\rangle[\hat{4}|p_{1\hat{5}9}|9\rangle[\hat{4}|p_{1\hat{5}9}|8\rangle[\hat{4}|p_{1\hat{5}9}|2\rangle} \\
&\times \frac{[\hat{4}|p_{1\hat{5}89}|2\rangle^3}{(\langle 3\hat{4}\rangle+\alpha_2\langle 3\hat{5}\rangle)(\langle \hat{4}7\rangle+\alpha_2\langle \hat{5}7\rangle)[\hat{4}|p_{12\hat{5}89}|8\rangle[\hat{4}|p_{12\hat{5}89}|7\rangle[\hat{4}|p_{12\hat{5}89}|3\rangle} \\
&\times\delta^{1\times 4}\{\tilde{\eta}_1+\frac{[\hat{4}|p_{1\hat{5}9}|9\rangle}{[\hat{4}|p_{1\hat{5}9}|1\rangle}\tilde{\eta}_9+\frac{[\hat{4}|p_{1\hat{5}9}|\hat{5}\rangle}{[\hat{4}|p_{1\hat{5}9}|1\rangle}[\tilde{\eta}_5-\alpha_2(\tilde{\eta}_4-\alpha_1\tilde{\eta}_5)]\} \\
&\times\Bigg\{\delta^{1\times 4}\{\tilde{\eta}_2+\frac{[\hat{4}|p_{12\hat{5}89}|1\rangle}{[\hat{4}|p_{12\hat{5}89}|2\rangle}\tilde{\eta}_1+\frac{[\hat{4}|p_{12\hat{5}89}|\hat{5}\rangle}{[\hat{4}|p_{12\hat{5}89}|2\rangle}[\tilde{\eta}_5-\alpha_2(\tilde{\eta}_4-\alpha_1\tilde{\eta}_5)]\} \\
&\qquad+\frac{[\hat{4}|p_{12\hat{5}89}|8\rangle}{[\hat{4}|p_{12\hat{5}89}|2\rangle}\tilde{\eta}_8+\frac{[\hat{4}|p_{12\hat{5}89}|9\rangle}{[\hat{4}|p_{12\hat{5}89}|2\rangle}\tilde{\eta}_9]\Bigg\}\times\delta^{2\times 4}(\Sigma\lambda_i\tilde{\eta}_i)
\end{aligned}
\tag{4.23}
$$

Integrate over both $I$ in the amplitude's expression, the amplitude becomes

$$
\int\frac{d\alpha_1}{\alpha_1}\frac{d\alpha_2}{\alpha_2}\delta[(I_1+p_1+p_9+l)^2]\delta[(I_1+I_2+p_2+p_8)^2]\mathcal{A}_4^2\mathcal{A}_4^2\mathcal{A}_4^2 \tag{4.24}
$$

Notice that the Dirac delta functions are both quadratic equations, whose factorization give two first-order equations of $\alpha$. Since $\alpha_2$ can be obtained from $\alpha_1$, we can first integrate over $\alpha_2$ and then factorize the remaining quadratic equation before integrating over $\alpha_1$. The calculation result is then

$$
\begin{aligned}
\frac{1}{S}\equiv\int\frac{d\alpha_1}{\alpha_1}\frac{d\alpha_2}{\alpha_2}\delta[(I_1+p_1+p_9+l)^2]\delta[(I_1+I_2+p_2+p_8)^2]&=\frac{1}{s_{1\hat{5}9}} \\
\times\frac{\langle\hat{5}|p_{19}|\hat{4}]}{\langle 4|p_{19}\circ(p_{28}\circ p_{19}-p_{28}\circ p_4-p_{28}^2)|5]}& \\
\times\frac{1}{|\alpha_{1+}-\alpha_{1-}|}(\frac{1}{\alpha_{1+}}+\frac{1}{\alpha_{1-}})&
\end{aligned}
\tag{4.25}
$$

The amplitude of twisted $\mathcal{A}_8^4$ is thus clear after substituting $\alpha_1$'s two values into the expression. The final amplitude of box chain requires two more operations. One is to add up both twisted $\mathcal{A}_8^4$'s amplitude and the other is to relabel the diagram in cyclic order. The amplitude of box chain $\mathcal{A}_8^4$ finally reads

$$
\mathcal{A}_8^4=-\mathcal{C}(1+r_{45})\frac{\mathcal{A}_4^2\mathcal{A}_4^2\mathcal{A}_4^2}{S}, \tag{4.26}
$$

where operator $r_{ij}$ switches label i and j in amplitudes and operator $\mathcal{C}$ relabels the whole diagram to cyclic order.

We stress that for $\mathcal{A}_n^k$ with large $n$, in particular, the calculation process can be greatly reduced based on the BCFW constructed form. The scattering amplitude of an one-loop leading singularitiy—be it planar or nonplanar—can be otained almost as conveniently as in tree level diagrams.

## 5 conclusion and outlook

In this paper we study nonplanar leading singularities. We focus on the BCFW decomposition chain, the top-form and the explicit amplitudes of nonplanar leading singularities.

We construct the BCFW decomposition chain by introducing a *cut* on one internal line and write down the permutation of the unglued planar diagram . We name it the marked permutation. Like permutation working on planar graphs, marked permutation labels the BCFW decomposition chain in a remarkably simple way. The marked permutation of one-loop leading singularities falls into one of three categories: External Line Pair, Black-White Chain and Box Chain.

- In External Line Pair cases, the loop is unfolded and the graph becomes identity upon removing a series of BCFW-bridge.
- In Black-White Chain cases, the graph can be transformed into external line pair type by performing a $U(1)$ decoupling relation of three-point amplitudes on a vertex.
- In Box chain cases, the graph can also be transformed into external line pair type by performing a $U(1)$ decoupling relation of four-point amplitudes on a box.

Therefore we can reconstruct any one-loop leading singularity and its d$log$ form from identity, utilizing marked permutation, BCFW-bridges and $U(1)$ decoupling relation.

Marked permutation unveils the top-forms of nonplanar leading singularities. The integration contour in top-form integral is determined by the geometric constraints on the Grassmannian manifold. For general on-shell diagrams, BCFW decomposition chain can be utilized to determine all possible linear dependences among the columns of Grassmannian matrix $C$. This indicates the correlations between BCFW decomposition and "matroid stratification" [80], which will be further discussed in our future work. The integrand of nonplanar top-form also needs to be constructed from scratch.

We attach a non-adjacent bridge on a planar diagram to construct a nonplanar diagram, and derive the new integrand as well as the integration contour. We can finally construct the top-form for any nonplanar leading singularities by adding BCFW-bridges subsequently. For MHV diagrams, the top-form can be further simplified into the summation of several planar diagrams. This conclusion holds for all loop conditions. At one-loop level, the reduction process corresponds to the KK relations [79]. In one-loop NMHV and $\mathrm{N}^2$MHV cases nonplanar top-forms can also be obtained and there are clues that the integrands can be reduced to several planar-like diagrams. We shall resolve the simplifications of $\mathrm{N}^k$MHV top-forms in our future work.

We then calculate nonplanar one-loop leading singularities explicitly in the BCFW constructed form. We utilize the marked permutation to categorize the poles into two types: local poles and nonlocal poles. We then define the canonical order according to the pole types:

- Bridge decompositions mustn't cross any already-obtained local pole;
- Disconnected graph except for identity is forbidden;

and obtained an explicit BCFW chain to decompose the one-loop leading singularities in an extremely efficient manner. We then calculate the delta functions of each type of poles and the supermomentum factors of the amplitudes. We prove that under canonical order the two type of poles are respectively analogous to on-shell propagators and three-point vertices in BCFW recursion relation of tree-level amplitudes. The BCFW constructed form of one decomposition chain is:

$$\begin{aligned}\mathcal{A}_n^k = &\int \frac{d\alpha_1}{\alpha_1} \wedge \cdots \wedge \frac{d\alpha_{2n-4}}{\alpha_{2n-4}} \prod_{h=1}^{n_p} \delta(\hat{p}_h^2)\delta^{2\times 2}(\lambda\cdot\tilde{\lambda})\delta^{2\times 4}(\lambda\cdot\tilde{\eta}) \\ &\times \prod_{i=1}^{n_w} \delta\left([i\ I_w]^2[i\ i-1]\alpha_i - \frac{1}{\overline{\mathcal{A}}_{W_i}}\right)[i-1\ i]^4 \\ &\times \prod_{j=1}^{n_b} \delta\left(\langle j\ I_b\rangle^2\langle j\ j+1\rangle\alpha_j - \frac{1}{\overline{\mathcal{A}}_{B_j}}\right)\langle I_b\ j+1\rangle^4\delta^{1\times 4}\left(\tilde{\eta}_j + \frac{\langle I\ j\rangle}{\langle I\ j+1\rangle}\tilde{\eta}_{j+1}\right) \\ &\times \delta(\alpha-1)\,. \end{aligned} \tag{5.1}$$

The construction of nonplanar amplitudes for leading singularities itself lends hope to finding the all loop integrands, as long as all propagators are obtained. More ideas and methods in topology are called for while dealing with higher-loop nonplanar amplitudes. In the next paper we will provide a systematic method to solve the all loop

amplitudes utilizing bipartite on-shell diagrams. Besides, the top-form of the nonplanar leading singularity requires further studies in the level of N$^k$MHV amplitude. We will probably find that N$^k$MHV top-form can also be simplified to several planar-like top-forms, or it is the sum of several N$^k$MHV top-forms that can be finally reduced as we wish. These expected discoveries will dig a new path for constructing the all loop scattering amplitudes. Last but not the least we shall apply our methodology to $\mathcal{N} < 4$ SYM or gauge theories in other dimensions.

## Acknowledgments

We thank Peizhi Du, Shuyi Li and Hanqing Liu for constructive discussion. Yuan Xin thanks Bo Feng for introducing the background on the recent developments of scattering amplitude. This research project has been supported by the Fundamental Research Funds for the Central Universities under contract 020414340080, the Youth Foundation of China under contract 11405084, the Jiangsu Ministry of Science and Technology under contract BK20131264 and by the Swedish Research Links programme of the Swedish Research Council (Vetenskapsradets generella villkor) under contract 348-2008-6049. We also acknowledge 985 Grants from the Ministry of Education, and the Priority Academic Program Development for Jiangsu Higher Education Institutions (PAPD).

## A BCFW-bridge decomposition to three basic types of diagrams

As discussed in [43], any planar on-shell diagram can be decomposed to identities by adjacent BCFW-bridge decomposition. For nonplanar diagrams of leading singularities, BCFW-bridge decomposition still works well. We can cut a loop line or move a partial graph from the nonplanar leading singularity such that the unglued or partial graph is planar with two marked unglued lines $A, \bar{A}$. Then the graph can be characterized by the marked permutations $\{\sigma(a_1)\cdots\sigma(a_i)\sigma(A)\sigma(b_1)\cdots\sigma(b_j)\sigma(\bar{A})\}$. It can be classified to three types according to the marked permutation as follows

**(1)** $\sigma(A) \neq \bar{A}$ && $\sigma(\bar{A}) \neq A$;

**(2)** $\sigma(A) = \bar{A}$ && $\sigma(\bar{A}) \neq A$, or $\sigma(\bar{A}) = A$ && $\sigma(A) \neq \bar{A}$;

**(3)** $\sigma(A) = \bar{A}$ && $\sigma(\bar{A}) = A$.

**Theorem 1** *The unglued or partial graph can be decomposed to three basic types of on-shell diagrams by removing adjacent BCFW-bridges, giving the corresponding permutations as*

***(1)*** *External Line Pair*

- $$\sigma = \begin{pmatrix} a_1 & a_2 & \cdots & a_{m-1} & a_m & A & b_1 & b_2 & \cdots & b_{m-1} & b_m & \bar{A} \\ \downarrow & \downarrow & \downarrow & \downarrow & \downarrow & \downarrow & \downarrow & \downarrow & \downarrow & \downarrow & \downarrow & \downarrow \\ \bar{A} & b_{m-1} & \cdots & b_2 & b_1 & a_m & A & a_{m-1} & \cdots & a_2 & a_1 & b_m \end{pmatrix},$$

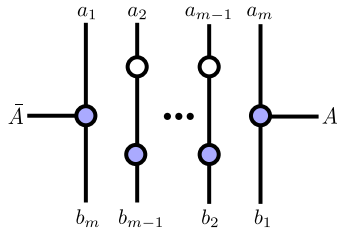


- $$\sigma = \begin{pmatrix} a_1 & a_2 & \cdots & a_m & A & b_1 & b_2 & \cdots & b_m & \bar{A} \\ \downarrow & \downarrow & \downarrow & \downarrow & \downarrow & \downarrow & \downarrow & \downarrow & \downarrow & \downarrow \\ \bar{A} & b_m & \cdots & b_2 & b_1 & A & a_m & \cdots & a_2 & a_1 \end{pmatrix},$$

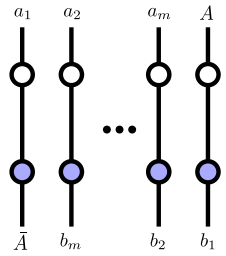


- $$\sigma = \begin{pmatrix} a_1 & a_2 & \cdots & a_{m-1} & a_m & A & b_1 & \cdots & b_{m-2} & b_{m-1} & \bar{A} \\ \downarrow & \downarrow & \downarrow & \downarrow & \downarrow & \downarrow & \downarrow & \downarrow & \downarrow & \downarrow & \downarrow \\ \bar{A} & b_{m-2} & \cdots & b_1 & A & a_m & a_{m-1} & \cdots & a_2 & a_1 & b_{m-1} \end{pmatrix}.$$

- $$\sigma = \begin{pmatrix} a_1 & a_2 & \cdots & a_{m-1} & a_m & A & b_1 & b_2 & \cdots & b_{m-1} & \bar{A} \\ \downarrow & \downarrow & \downarrow & \downarrow & \downarrow & \downarrow & \downarrow & \downarrow & \downarrow & \downarrow & \downarrow \\ \bar{A} & b_{m-1} & \cdots & b_2 & b_1 & a_m & A & a_{m-1} & \cdots & a_2 & a_1 \end{pmatrix}.$$

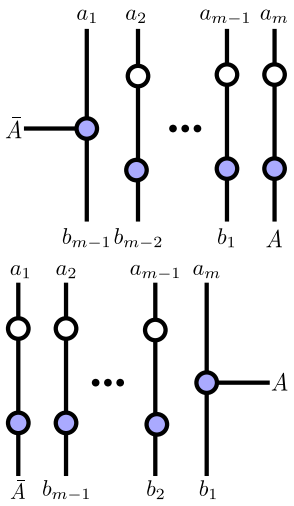


- $$\sigma = \begin{pmatrix} a_1 & a_2 & \cdots & a_{m-1} & a_m & A & b_1 & \cdots & b_{m-2} & \bar{A} \\ \downarrow & \downarrow & \downarrow & \downarrow & \downarrow & \downarrow & \downarrow & \downarrow & \downarrow & \downarrow \\ \bar{A} & b_{m-2} & \cdots & b_1 & A & a_m & a_{m-1} & \cdots & a_2 & a_1 \end{pmatrix}.$$

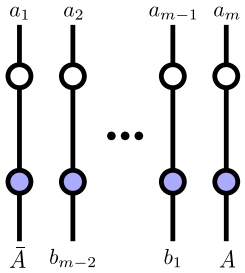


- *We can also replace the three point black vertexes in above cases by white ones.*

*(2) Black-White Chain*

- $$\sigma = \begin{pmatrix} a_1 & a_2 & \cdots & a_{m-1} & a_m & A & b_1 & b_2 & \cdots & b_m & \bar{A} \\ \downarrow & \downarrow & \downarrow & \downarrow & \downarrow & \downarrow & \downarrow & \downarrow & \downarrow & \downarrow & \downarrow \\ b_m & b_{m-1} & \cdots & b_2 & b_1 & \bar{A} & A & a_m & \cdots & a_2 & a_1 \end{pmatrix}.$$

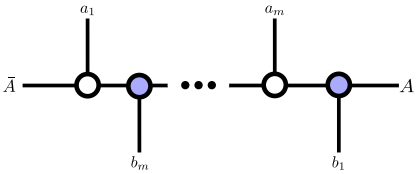

- $$\sigma = \begin{pmatrix} a_1 & \cdots & a_{m-1} & a_m & A & b_1 & \cdots & b_m & \bar{A} \\ \downarrow & \downarrow & \downarrow & \downarrow & \downarrow & \downarrow & \downarrow & \downarrow & \downarrow \\ b_{m-1} & \cdots & b_1 & A & \bar{A} & a_m & \cdots & a_1 & b_m \end{pmatrix}.$$

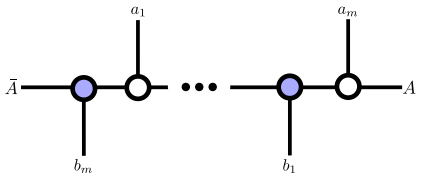


- $$\sigma = \begin{pmatrix} a_1 & \cdots & a_{m-1} & a_m & A & b_1 & \cdots & b_{m-1} & \bar{A} \\ \downarrow & \downarrow & \downarrow & \downarrow & \downarrow & \downarrow & \downarrow & \downarrow & \downarrow \\ b_{m-1} & \cdots & b_1 & A & \bar{A} & a_m & \cdots & a_2 & a_1 \end{pmatrix}.$$

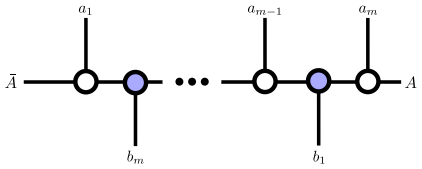


- $$\sigma = \begin{pmatrix} a_1 & \cdots & a_m & A & b_1 & \cdots & b_{m-1} & b_m & \bar{A} \\ \downarrow & \downarrow & \downarrow & \downarrow & \downarrow & \downarrow & \downarrow & \downarrow & \downarrow \\ b_m & \cdots & b_1 & a_m & a_{m-1} & \cdots & a_1 & \bar{A} & A \end{pmatrix}.$$

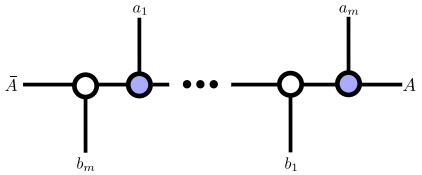


- $$\sigma = \begin{pmatrix} a_1 & a_2 & \cdots & a_m & A & b_1 & \cdots & b_m & \bar{A} \\ \downarrow & \downarrow & \downarrow & \downarrow & \downarrow & \downarrow & \downarrow & \downarrow & \downarrow \\ \bar{A} & b_m & \cdots & b_2 & b_1 & a_m & \cdots & a_1 & A \end{pmatrix}.$$

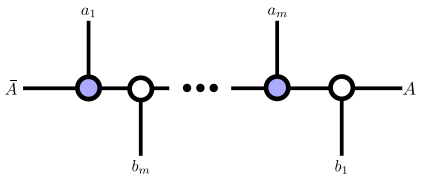

•

$$\sigma = \begin{pmatrix} a_1 & a_2 & \cdots & a_m & A & b_1 & \cdots & b_{m-1} & \bar{A} \\ \downarrow & \downarrow & \downarrow & \downarrow & \downarrow & \downarrow & \downarrow & \downarrow & \downarrow \\ \bar{A} & b_{m-1} & \cdots & b_1 & a_m & a_{m-1} & \cdots & a_1 & A \end{pmatrix}.$$

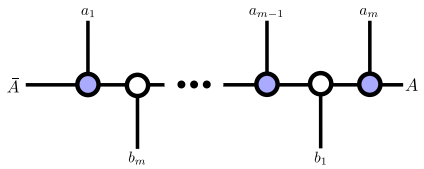


*(3) Box Chain*

$$\sigma = \begin{pmatrix} a_1 & \cdots & a_m & A & b_1 & \cdots & b_m & \bar{A} \\ \downarrow & \downarrow & \downarrow & \downarrow & \downarrow & \downarrow & \downarrow & \downarrow \\ b_m & \cdots & b_1 & \bar{A} & a_m & \cdots & a_1 & A \end{pmatrix}.$$

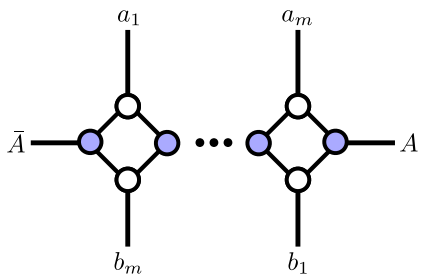


Proof: We can label the $n$ external lines $\{a_1, \cdots, a_i, A, b_1, \cdots, b_j, \bar{A}\}$ of the graph in the cyclic order as $\{1 \cdots i, i+1, i+2 \cdots i+j+1, i+j+2\}$. We call the lines $\{1 \cdots i\}$ and lines $\{i+2 \cdots i+j+1\}$ as up-lines and down-lines respectively. As discussed in section **??**, in the cyclic order the adjacent BCFW-bridges can be sorted into two types: WB-bridge and BW-bridge. After removing the WB-bridge $\mathcal{B}_{wb}(k, k+1)$ or BW-bridge $\mathcal{B}_{bw}(k, k+1)$, the modification on the permutation is $\sigma \to \sigma' = Z_2(k, k+1) \cdot \sigma$ or $\sigma \to \sigma' = Z_2(\sigma^{-1}(k), \sigma^{-1}(k+1)) \cdot \sigma$ respectively, where $Z_2(k, k+1)$ is a $Z_2$ permutation on line $k$ and $k+1$. It is obvious that the diagram will contain a WB-bridge $\mathcal{B}_{wb}(k, k+1)$ in the diagram if $\sigma(k) < \sigma(k+1)$ or a BW-bridge $\mathcal{B}_{bw}(k, k+1)$ if $\sigma^{-1}(k) < \sigma^{-1}(k+1)$.

**Under WB-bridge decompositions, an up-line $k$ with $\sigma^{-1}(k) \in \{1, \cdots, i\}$ or a down-line $k$ with $\sigma^{-1}(k) \in \{i+2, \cdots, i+j+1\}$ can be transformed to identity.** For two up-lines $k_b = \sigma^{-1}(k_e), k_e$, we only prove reductively for the case with $k_e > k_b$ that the $k_e$ can be transformed to identity by removing WB-bridges. The $k_e < k_b$ case is similar.

First For the case $k_e - k_b = 1$. Since

$$\sigma(k_e) = \begin{cases} k_s \ (\text{if } k_s > k_e) \\ k_s + n \ (\text{if } k_s < k_e) \end{cases},$$

it is obvious that $\sigma(k_b) < \sigma(k_e)$. After removing the BW-bridge on lines $(k_b, k_e)$, the resulting permutation is $\sigma'(k_e) = k_e$ which means label $k_e$ has become identity.

Second For the case $k_e - k_b = 2$. Due to the same reason we have $\sigma(k_b) < \sigma(k_e)$ and $\sigma(k_b) < \sigma(k_e - 1)$. Then we can remove both the $\mathcal{B}_{bw}(k_b, k_e - 1)$ bridge and the $\mathcal{B}_{bw}(k_e - 1, k_e)$ bridge. The resulting permutation is $\sigma'(k_e) = k_e$.

Third For the case $k_e - k_b = 3$. We find $\sigma(k_b) < \sigma(k_e)$, $\sigma(k_b) < \sigma(k_e - 1)$ and

$$\sigma(k_e - 2) = \begin{cases} k_s & (\text{if } k_s > k_e) \\ k_s + N & (\text{if } k_s < k_e - 2) \\ k_e - 1 & (\text{others}). \end{cases}$$

If $\sigma(k_e - 2) \neq k_e - 1$, we can remove the BW-bridges consecutively and transform $k_e$ to identity. If $\sigma(k_e - 2) = k_e - 1$, we can set $k'_b = k_e - 2$ and $k'_e = k_e - 1$. Then according to the results in the first step, label $k_e - 1$ can be transformed to identity. Then we can remove the identity line from the diagram. According to the results in the second step, line $k_e$ can be transformed to identity.

Fourth We assume that all the label $k_e$ can be transformed to identity if $\sigma(k'_b) = k'_e$ and $k'_e - k'_b \leq n - 1$. Then we discuss the case $\sigma(k_b) = k_e$ and $k_e - k_b = n$. For the lines $k_i \in (k_b, k_e)$,

$$\sigma(k_i) = \begin{cases} k_s & (\text{if } k_s > k_e) \\ k_s + N & (\text{if } k_s < k_i) \\ k_s & (\text{if } k_i < k_s < k_e). \end{cases}$$

It is obvious that if there are some $k_i$'s such that $\sigma(k_i) = k_s \in (k_i, k_e)$, line $k_s$ can be removed from the whole diagram according to the reductive assumption. After removing all such lines, we can obtain a diagram with permutation $\sigma(k'_b) = k'_e$ and $k'_e - k'_b \leq n - 1$. Hence label $k_e$ can be transformed to identity in the remaining permutations. If all the lines $k_i$ are permuted to $k_s > k_e$ or $k_s < k_i$. Then $\sigma(k_b) < \sigma(k_i)$. We can remove the BW-bridges to transform label $k_e$ to identity. Similar proofs are suitable for the down-set lines.

As a result, after removing adjacent WB-bridges, an up-line $k$ with $1 < \sigma^{-1}(k) < i$ or a down-line $k$ with $i + 2 < \sigma^{-1}(k) < i + j + 1$ can be separated from the other

parts for they are identity lines after decomposition. If we drop these external lines, we can relabel all the remaining external lines as $\{1\cdots m, m+1, m+2, \cdots, m+n+1, m+n+2\}$. And we label the resulting permutation as $\bar{\sigma}$. Without losing generality, we can set $n \leq m$. Since the remaining n up-lines will permute to down-lines or 2 gluing lines while the remaining m down-lines will permute to up-lines or 2 gluing lines, there are only three cases: $n = m$, $n = m-1$ and $n = m-2$. Then, the three types can be characterized more finely:

**(1)** $\bar{\sigma}(A) \neq \bar{A}$ && $\bar{\sigma}(\bar{A}) \neq A$

- n=m-2;
- n=m-1;
- n=m;

**(2)** $\bar{\sigma}(A) = \bar{A}$ && $\bar{\sigma}(\bar{A}) \neq A$ or $\bar{\sigma}(\bar{A}) = A$ && $\bar{\sigma}(A) \neq \bar{A}$

- n=m-1;
- n=m;

**(3)** $\bar{\sigma}(A) = \bar{A}$ && $\bar{\sigma}(\bar{A}) = A$, n=m.

**Removing bridge does not change the fine types** As discussed above, when removing a WB-bridge between external lines $k_x$ and $k_y$, we exchange $\sigma(x)$ with $\sigma(y)$. When removing a Black-White bridge between external lines $x$ and $y$, we exchange $\sigma^{-1}(x)$ with $\sigma^{-1}(y)$. Therefore, for a certain on-shell diagram, since the operation of removing bridges related with gluing lines is forbidden, the permutations of two gluing lines remain unchanged. Hence removing adjacent BCFW-bridges will not change the fine types.

After removing all the adjacent BCFW-bridges, we find that the final basic permutation $\bar{\sigma}$ will have the properties as following:

- $\{\bar{\sigma}(1), \cdots, \bar{\sigma}(m)\}$ and $\{\bar{\sigma}(m+2), \cdots, \bar{\sigma}(m+n+1)\}$ are in the descending order respectively.

  If the permutations above are not in a descending order, supposing $x$ and $y$ are two up-lines with $x < y$ and $\bar{\sigma}(x) < \bar{\sigma}(y)$, there must be adjacent BCFW-bridges between $x$ and $y$ that can be removed. Specifically, there must exist two adjacent external lines $p$ and $p+1$ with $\bar{\sigma}(p) < \bar{\sigma}(p+1)$. So we can remove these bridges

until $\bar{\sigma}(x) < \bar{\sigma}(y)$ for every two up-lines $x$ and $y$. The same conclusion holds for down-lines.

- $\bar{\sigma}(A) = \bar{A}$ or $a_m$ or $b_1$, $\bar{\sigma}(\bar{A}) = A$ or $a_1$ or $b_n$.

  If $\bar{\sigma}(A) = a_x$ with $a_1 \leq a_x \leq a_{m-1}$, we can find $a_{x+1}$ in the set $\{\bar{\sigma}(b_1), \cdots, \bar{\sigma}(b_n), \bar{\sigma}(\bar{A})\}$. Then we can remove the adjacent BW-bridge on line $a_x, a_{x+1}$. It contradicts the precondition that we have already removed all the bridges. Similarly we can prove $\bar{\sigma}(A)$ does not equal to $b_x$ with $b_2 \leq b_x \leq b_n$. Hence $\bar{\sigma}(A) = \bar{A}$ or $a_m$ or $b_1$. Similar proof holds for $\bar{\sigma}(\bar{A}) = A$ or $a_1$ or $b_n$.

Finally, we can obtain the allowed permutations for each type of $\bar{\sigma}$. We can see that for basic type (1), the diagram is composed of Black-White pairs. It may also contain three-point amplitudes with one gluing lines, which can be separated by removing adjacent BCFW-bridges. For type (2) the diagram is composed of Black-White chain. As for type (3), the diagram is a box chain. Therefore, three basic types of permutations correspond to *Black-White Pairs*, *Black-White Chain* and *Box Chain* respectively. Their difference simply depends on the permutations of the gluing lines. □

## B Geometry and Permutation

In this section we discuss the linear relations among columns of $C$, which yields the submanifold $\Gamma$. General nonplanar on-shell diagrams can be built-up by gluing the non-neighboring line of a certain unglued diagram. Conversely, a nonplanar diagram can be transformed into a unglued diagram after cutting one internal on-shell line. We shall investigate in detail the relationship between the gluing process and the unglued grassmannian matrix using the unglued permutations. It will unveil the geometrical associations between nonplanar and planar diagrams.

The Grassmannian of a diagram encodes the linear relations among the external lines. If we glue two external lines in an on-shell diagram, the Grassmannian matrix $C \in G(k, n)$ become $\widehat{C} \in G(k-1, n-2)$. We use numbers $1, 2 \cdots n$ to mark the external line and label the glued line as "i" and "n". In Grassmannian matrix, the

gluing process is

$$C=\begin{pmatrix} a_{1,1} & \dots & a_{1,i} & \dots & a_{1,n} \\ a_{2,1} & \dots & a_{2,i} & \dots & a_{2,n} \\ \vdots & \ddots & \vdots & \ddots & \vdots \\ a_{k-1,1} & \dots & a_{k-1,i} & \dots & a_{k-1,n} \\ a_{k,1} & \dots & a_{k,i} & \dots & a_{k,n} \end{pmatrix} \to \begin{pmatrix} a_{1,1} & \dots & a_{1,i}+a_{1,n} & \dots & a_{1,n-1} \\ a_{2,1} & \dots & a_{2,i}+a_{2,n} & \dots & a_{2,n-1} \\ \vdots & \ddots & \vdots & \ddots & \vdots \\ a_{k-1,1} & \dots & a_{k-1,i}+a_{k-1,n} & \dots & a_{k-1,n-1} \\ a_{k,1} & \dots & a_{k,i}+a_{k,n} & \dots & a_{k,n-1} \end{pmatrix} \tag{B.1}$$

Without losing any generality, we can choose $a_{1,i}+a_{1,n}\neq 0$, Under $GL(k)$ transformation all other elements in the same column become zero.

$$\begin{pmatrix} a_{1,1} & \dots & a_{1,i}+a_{1,n} & \dots & a_{1,n-1} \\ b_{2,1} & \dots & 0 & \dots & b_{2,n-1} \\ \vdots & \ddots & \vdots & \ddots & \vdots \\ b_{k-1,1} & \dots & 0 & \dots & b_{k-1,n-1} \\ b_{k,1} & \dots & 0 & \dots & b_{k,n-1} \end{pmatrix} \tag{B.2}$$

The Grassmannian matrix of glued diagram can be obtained by deleting the first row and $i$th column:

$$\widehat{C}=\begin{pmatrix} b_{2,1} & \dots & b_{2,i-1} & b_{2,i+1} & \dots & b_{2,n} \\ \vdots & \ddots & \vdots & \vdots & \ddots & \vdots \\ b_{k-1,1} & \dots & b_{k-1,i-1} & b_{k-1,i+1} & \dots & b_{k-1,n} \\ b_{k,1} & \dots & b_{k,i-1} & b_{k,i+1} & \dots & b_{k,n} \end{pmatrix} \tag{B.3}$$

Combine Eq. B.1, B.2 and B.3, minors of $\widehat{C}$ can be given in terms of the minors of $C$ according to:

$$(b_{m_1},b_{m_2},\dots,b_{m_k})|_{\widehat{C}}=\frac{1}{(a_{1,i}+a_{1,n})}(a_i+a_n,a_{m_1},a_{m_2},\dots,a_{m_k})|_C \tag{B.4}$$

Note that constraints in Grassmannian matrix are linear relations among several columns. These constraints are equivalent to zero minors. Thus according to Eq. B.4, we find $(b_{m_1},b_{m_2},\dots,b_{m_k})|_{\widehat{C}}=0$ implies $(a_i,a_{m_1},a_{m_2},\dots,a_{m_k})|_C+(a_i,a_{m_1},a_{m_2},\dots,a_{m_k})|_C=0$. With this relation, we can obtain the constraints in $\widehat{C}$ through studying the structure of $C$. Further, we can prove

$$\left.\begin{array}{l}(a_i,a_{m_1},a_{m_2},\dots,a_{m_k})|_C=0\\(a_n,a_{m_1},a_{m_2},\dots,a_{m_k})|_C=0\end{array}\right\}\Longleftrightarrow(b_{m_1},b_{m_2},\dots,b_{m_k})|_{\widehat{C}}=0 \tag{B.5}$$

To prove this relation, we write down the constraints $(a_i+a_n,a_{m_1},a_{m_2},\dots,a_{m_k})|_C=0$ explicitly:

$$e_{i+n}(a_i+a_n)+e_{m_1}a_{m_1}+e_{m_2}a_{m_2}+\dots+e_{m_k}a_{m_k}=0 \tag{B.6}$$

where $e_m$ are coefficients of column $a_m$ and they are not fixed before integration. If we assume that this relation can be generated by the linear combinations of other two linear relation for simply (for combinations of more than two linear relations can be analyzed step by step similarly):

$$\begin{aligned} e_i a_i + e_n a_n + e_{m_1} a_{m_1} + \cdots + e_{m_k} a_{m_k} + e_{m_{k+1}} a_{m_{k+1}} + \cdots + e_{m_{k+p}} a_{m_{k+p}} &= 0 \\ e'_i a_i + e'_n a_n + e'_{m_1} a_{m_1} + \cdots + e'_{m_k} a_{m_k} + e'_{m_{k+1}} a_{m_{k+1}} + \cdots + e'_{m_{k+p}} a_{m_{k+p}} &= 0 \end{aligned} \quad \text{(B.7)}$$

Multiply the first relation by coefficient $E$ and add it to the second relation, a new relation yields:

$$\begin{aligned} (Ee_i + e'_i)a_i + (Ee_n + e'_n)a_n + \cdots + (Ee_{m_{k+1}} + e'_{m_{k+1}})a_{m_{k+1}} \\ + \cdots + (Ee_{m_{k+p}} + e'_{m_{k+p}})a_{m_{k+p}} = 0 \end{aligned} \quad \text{(B.8)}$$

Combining the coefficients in Eq. B.8 and Eq. B.6, we have

$$\begin{aligned} (Ee_i + e'_i) - (Ee_n + e'_n) &= 0 \\ Ee_{m_{k+1}} + e'_{m_{k+1}} &= 0 \\ &\vdots \\ Ee_{m_{k+p}} + e'_{m_{k+p}} &= 0 \end{aligned} \quad \text{(B.9)}$$

Each $e_m = 0$ in Eq. B.6, B.8 and B.9 means that the linear relation does not involve $a_m$. If the coefficient is not zero, it is not fixed and we cannot impose extra constraints on them to make all equations linearly dependent. Since all such coefficients are not fixed, the equations are linearly independent. There are $p+1$ constraints but only one variable E. The only solution set to the equations is

$$\begin{aligned} E &= \frac{e'_n - e'_i}{e_i - e_n} \\ e_{m_{k+1}} &= \cdots = e_{m_{k+p}} = 0 \\ e'_{m_{k+1}} &= \cdots = e'_{m_{k+p}} = 0. \end{aligned}$$

These two linear relations further simplify Eq. B.7 to

$$\begin{pmatrix} e_i & e_n & e_{m_1} & e_{m_2} & \cdots & e_{m_k} \\ e'_i & e'_n & e'_{m_1} & e'_{m_2} & \cdots & e'_{m_k} \end{pmatrix} \begin{pmatrix} a_i \\ a_n \\ a_{m_1} \\ a_{m_2} \\ \vdots \\ a_{m_k} \end{pmatrix} = 0 \quad \text{(B.10)}$$

Through linear transformations, the coefficient matrix turns into

$$\begin{pmatrix} 1 & 0 & e*_{m_1} & e*_{m_2} & \cdots & e*_{m_k} \\ 0 & 1 & e*'_{m_1} & e*'_{m_2} & \cdots & e*'_{m_k} \end{pmatrix}$$

which are equivalent to two zero minors:

$$\begin{aligned} (a_i, a_{m_1}, a_{m_2}, \ldots, a_{m_k}) &= 0 \\ (a_n, a_{m_1}, a_{m_2}, \ldots, a_{m_k}) &= 0 \end{aligned} \tag{B.11}$$

Thus in order to generate Eq. B.6, we should send the above two minors to zero. Since all the constraints in Grassmannian matrix should be represented by these linear relations or their equivalent forms, this procedure is the only way to generate Eq. B.6. In conclusion, we have $(a_i, a_{m_1}, a_{m_2}, \ldots, a_{m_k})|_C = 0$ and $(a_n, a_{m_1}, a_{m_2}, \ldots, a_{m_k})|_C = 0$ if $(b_{m_1}, b_{m_2}, \ldots, b_{m_k})|_{\widehat{C}} = 0$. It is an important relation and can be used to search and determine the complete geometry information in the glued diagram.

To illustrate this procedure, we use $\mathcal{A}_6^3$ one-loop nonplanar diagram as an example.

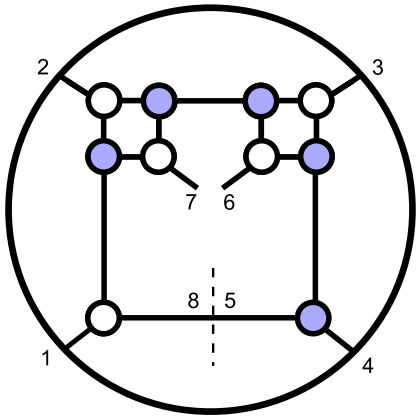


**Figure 22**. NonPlanar Diagram $\mathcal{A}_6^3$

Permutation of the planar diagram after cutting one internal line as shown in Fig. 22 is

$$\sigma = \begin{pmatrix} 1 & 2 & 3 & 4 & 5 & 6 & 7 & 8 \\ \downarrow & \downarrow & \downarrow & \downarrow & \downarrow & \downarrow & \downarrow & \downarrow \\ 8 & 7 & 6 & 5 & 9 & 11 & 10 & 12 \end{pmatrix}$$

The corresponding linear relations are

$$\begin{aligned} (2(3(4,5)^1 6)^2 7)^3|_C \\ (3(4,5)^1 6)^2|_C \\ (4,5)^1|_C \\ (7,8,1,2)^3|_C \end{aligned}$$

$(7,8,1,2)^3|_C$ means the matrix constituted by column $7,8,1,2$ in grassmannian matrix is of rank 3. So as the other three relations. If we glue back external lines 5 and 8 to form an internal line, column 5 and 8 will be eliminated. Every two relations will generate a new relation in the process. For example, $(4,5)^1|_C$ means $5 \in span\{4\}$, thus 5 can be used to eliminate 6 in relation $(3(4,5)^1 6)^2|_C$. The resulting new relation is $(3,4,6)^2|_C$. If both 1 and 6 exist in the two relations, like $(4,5)^1|_C$ and $(7,8,1,2)^3|_C$, the new relation should eliminate not only 5, but also 8. In this example, the new relation is $(4,7,1,2)^4|_C$. But what we really care are those relations in $\widehat{C}$ instead of $C$.

$$\begin{aligned}(8,4,7,1,2)^4|_C \cap (5,4,7,1,2)^4|_C &\Longrightarrow (4,7,1,2)^3|_{\widehat{C}} \\ (8,3,4,6)^3|_C \cap (5,3,4,6)^2|_C &\Longrightarrow (3,4,6)^2|_{\widehat{C}}\end{aligned}$$

Sort out all nontrivial($rank < 3$) relations, the only one left is $(3,4,6)^2|_{\widehat{C}}$.

For general one-loop nonplanar diagrams, the procedure of finding geometric constraints can be summarized as follows. First, choose an appropriate internal line to perform the "cut." Second, write down the linear relations in the planar diagram by permutation. The final step is to combine every two relations to generate a new one through the equivalence relation Eq. B.5. Keep searching all new relations until all independent constraints are exhausted. As long as the constraints we find in the unglued diagram are complete, the constraints after gluing found using this method are complete as well.

## References


[1] R. Britto, F. Cachazo, and B. Feng, *Computing one-loop amplitudes from the holomorphic anomaly of unitarity cuts*, *Phys. Rev. D* **71** (Jan., 2005) 025012, [hep-th/0410179].

[2] R. Britto, F. Cachazo, and B. Feng, *New recursion relations for tree amplitudes of gluons*, *Nuclear Physics B* **715** (May, 2005) 499–522, [hep-th/0412308].

[3] R. Britto, F. Cachazo, B. Feng, and E. Witten, *Direct Proof of the Tree-Level Scattering Amplitude Recursion Relation in Yang-Mills Theory*, *Physical Review Letters* **94** (May, 2005) 181602, [hep-th/0501052].

[4] B. Feng and M. Luo, *An introduction to on-shell recursion relations*, *Frontiers of Physics* **7** (Oct., 2012) 533–575, [arXiv:1111.5759].

[5] Z. Bern, L. Dixon, D. C. Dunbar, and D. A. Kosower, *One-loop n-point gauge theory amplitudes, unitarity and collinear limits*, *Nuclear Physics B* **425** (Aug., 1994) 217–260, [hep-ph/9403226].

[6] Z. Bern, L. Dixon, D. C. Dunbar, and D. A. Kosower, *Fusing gauge theory tree amplitudes into loop amplitudes*, *Nuclear Physics B* **435** (Feb., 1995) 59–101, [hep-ph/9409265].

[7] Z. Bern, L. J. Dixon, and V. A. Smirnov, *Iteration of planar amplitudes in maximally supersymmetric Yang-Mills theory at three loops and beyond*, *Phys. Rev. D* **72** (Oct., 2005) 085001, [hep-th/0505205].

[8] R. Britto, F. Cachazo, and B. Feng, *Generalized unitarity and one-loop amplitudes in N=4 super-Yang Mills*, *Nuclear Physics B* **725** (Oct., 2005) 275–305, [hep-th/0412103].

[9] R. Britto, E. Buchbinder, F. Cachazo, and B. Feng, *One-loop amplitudes of gluons in supersymmetric qcd*, *Phys. Rev. D* **72** (Sep, 2005) 065012.

[10] E. I. Buchbinder and F. Cachazo, *Two-loop amplitudes of gluons and octa-cuts in Script N = 4 super Yang-Mills*, *Journal of High Energy Physics* **11** (Nov., 2005) 36, [hep-th/0506126].

[11] J. Drummond, J. Henn, G. Korchemsky, and E. Sokatchev, *Generalized unitarity for N=4 super-amplitudes*, *Nucl.Phys.* **B869** (2013) 452–492, [arXiv:0808.0491].

[12] P. Mastrolia, E. Mirabella, G. Ossola, and T. Peraro, *Integrand-Reduction for Two-Loop Scattering Amplitudes through Multivariate Polynomial Division*, *Phys.Rev.* **D87** (2013) 085026, [arXiv:1209.4319].

[13] P. Mastrolia, E. Mirabella, G. Ossola, T. Peraro, and H. van Deurzen, *The Integrand Reduction of One- and Two-Loop Scattering Amplitudes*, *PoS* **LL2012** (2012) 028, [arXiv:1209.5678].

[14] P. Mastrolia, E. Mirabella, G. Ossola, and T. Peraro, *Multiloop Integrand Reduction for Dimensionally Regulated Amplitudes*, arXiv:1307.5832.

[15] H. van Deurzen, G. Luisoni, P. Mastrolia, E. Mirabella, G. Ossola, et al., *Multi-loop Integrand Reduction via Multivariate Polynomial Division*, arXiv:1312.1627.

[16] Z. Bern, M. Czakon, D. Kosower, R. Roiban, and V. Smirnov, *Two-loop iteration of five-point N=4 super-Yang-Mills amplitudes*, *Phys.Rev.Lett.* **97** (2006) 181601, [hep-th/0604074].

[17] J. J. Carrasco and H. Johansson, *Five-Point Amplitudes in N=4 Super-Yang-Mills Theory and N=8 Supergravity*, *Phys.Rev.* **D85** (2012) 025006, [arXiv:1106.4711].

[18] Z. Bern, L. Dixon, D. Kosower, R. Roiban, M. Spradlin, et al., *The Two-Loop Six-Gluon MHV Amplitude in Maximally Supersymmetric Yang-Mills Theory*, *Phys.Rev.* **D78** (2008) 045007, [arXiv:0803.1465].

[19] B. Eden, G. P. Korchemsky, and E. Sokatchev, *More on the duality*

*correlators/amplitudes*, *Physics Letters B* **709** (Mar., 2012) 247–253, [arXiv:1009.2488].

[20] B. Eden, P. Heslop, G. P. Korchemsky, and E. Sokatchev, *The super-correlator/super-amplitude duality: Part I*, *Nuclear Physics B* **869** (Apr., 2013) 329–377, [arXiv:1103.3714].

[21] B. Eden, P. Heslop, G. P. Korchemsky, and E. Sokatchev, *The super-correlator/super-amplitude duality: Part II*, *Nuclear Physics B* **869** (Apr., 2013) 378–416, [arXiv:1103.4353].

[22] F. Cachazo, *Sharpening The Leading Singularity*, *ArXiv e-prints* (Mar., 2008) [arXiv:0803.1988].

[23] N. Kanning, T. Lukowski, and M. Staudacher, *A shortcut to general tree-level scattering amplitudes in $\mathcal{N} = 4$ SYM via integrability*, *Fortsch.Phys.* **62** (2014) 556–572, [arXiv:1403.3382].

[24] A. Ochirov, *Scattering amplitudes in gauge theories with and without supersymmetry*, arXiv:1409.8087.

[25] J. Broedel, M. de Leeuw, and M. Rosso, *A dictionary between R-operators, on-shell graphs and Yangian algebras*, *JHEP* **1406** (2014) 170, [arXiv:1403.3670].

[26] J. Broedel, M. de Leeuw, and M. Rosso, *Deformed one-loop amplitudes in $N = 4$ super-Yang-Mills theory*, arXiv:1406.4024.

[27] N. Beisert, J. Broedel, and M. Rosso, *On yangian-invariant regularization of deformed on-shell diagrams in $\mathcal{N} = 4$ super-yang-mills theory*, *Journal of Physics A: Mathematical and Theoretical* **47** (2014), no. 36 365402.

[28] D. Chicherin, S. Derkachov, and R. Kirschner, *Yang-baxter operators and scattering amplitudes in super-yang-mills theory*, *Nuclear Physics B* **881** (2014), no. 0 467 – 501.

[29] J. Drummond, J. Henn, G. Korchemsky, and E. Sokatchev, *Dual superconformal symmetry of scattering amplitudes in N=4 super-Yang-Mills theory*, *Nucl.Phys.* **B828** (2010) 317–374, [arXiv:0807.1095].

[30] J. Drummond and J. Henn, *All tree-level amplitudes in N=4 SYM*, *JHEP* **0904** (2009) 018, [arXiv:0808.2475].

[31] J. M. Drummond, J. M. Henn, and J. Plefka, *Yangian symmetry of scattering amplitudes in N=4 super Yang-Mills theory*, *JHEP* **0905** (2009) 046, [arXiv:0902.2987].

[32] A. Brandhuber, P. Heslop, and G. Travaglini, *Proof of the Dual Conformal Anomaly of One-Loop Amplitudes in N=4 SYM*, *JHEP* **0910** (2009) 063, [arXiv:0906.3552].

[33] N. Arkani-Hamed, F. Cachazo, and J. Kaplan, *What is the simplest quantum field theory?*, *Journal of High Energy Physics* **9** (Sept., 2010) 16, [arXiv:0808.1446].

[34] F. Cachazo and D. Skinner, *On the structure of scattering amplitudes in N=4 super Yang-Mills and N=8 supergravity*, *ArXiv e-prints* (Jan., 2008) [arXiv:0801.4574].

[35] Z. Bern, J. J. M. Carrasco, H. Johansson, and D. A. Kosower, *Maximally supersymmetric planar Yang-Mills amplitudes at five loops*, *Phys. Rev. D* **76** (Dec., 2007) 125020, [arXiv:0705.1864].

[36] M. Spradlin, A. Volovich, and C. Wen, *Three-Loop Leading Singularities and BDS Ansatz for Five Particles*, *Phys.Rev.* **D78** (2008) 085025, [arXiv:0808.1054].

[37] N. Arkani-Hamed, F. Cachazo, C. Cheung, and J. Kaplan, *The S-matrix in twistor space*, *Journal of High Energy Physics* **3** (Mar., 2010) 110, [arXiv:0903.2110].

[38] M. F. Paulos and B. U. W. Schwab, *Cluster Algebras and the Positive Grassmannian*, *JHEP* **1410** (2014) 31, [arXiv:1406.7273].

[39] Y. Bai and S. He, *The Amplituhedron from Momentum Twistor Diagrams*, arXiv:1408.2459.

[40] L. Ferro, T. Lukowski, and M. Staudacher, *N=4 Scattering Amplitudes and the Deformed Grassmannian*, arXiv:1407.6736.

[41] S. Franco, D. Galloni, A. Mariotti, and J. Trnka, *Anatomy of the Amplituhedron*, arXiv:1408.3410.

[42] H. Elvang, Y.-t. Huang, C. Keeler, T. Lam, T. M. Olson, et al., *Grassmannians for scattering amplitudes in 4d $\mathcal{N} = 4$ SYM and 3d ABJM*, arXiv:1410.0621.

[43] N. Arkani-Hamed, J. L. Bourjaily, F. Cachazo, A. B. Goncharov, A. Postnikov, et al., *Scattering Amplitudes and the Positive Grassmannian*, arXiv:1212.5605.

[44] S. Franco, D. Galloni, and A. Mariotti, *The Geometry of On-Shell Diagrams*, arXiv:1310.3820.

[45] H. Elvang, D. Z. Freedman, and M. Kiermaier, *Dual conformal symmetry of 1-loop NMHV amplitudes in N=4 SYM theory*, *JHEP* **1003** (2010) 075, [arXiv:0905.4379].

[46] L. Dolan, C. R. Nappi, and E. Witten, *A relation between approaches to integrability in superconformal Yang-Mills theory*, *Journal of High Energy Physics* **10** (Oct., 2003) 17, [hep-th/0308089].

[47] L. Dolan, C. R. Nappi, and E. Witten, *Yangian Symmetry in D=4 Superconformal Yang-Mills Theory*, in *Quantum Theory and Symmetries* (P. C. Argyres, T. J. Hodges, F. Mansouri, J. J. Scanio, P. Suranyi, and L. C. R. Wijewardhana, eds.), pp. 300–315, Oct., 2004. hep-th/0401243.

[48] N. Beisert, J. Broedel, and M. Rosso, *On Yangian-invariant regularisation of deformed on-shell diagrams in N=4 super-Yang-Mills theory*, *ArXiv e-prints* (Jan., 2014) [arXiv:1401.7274].

[49] R. Frassek, N. Kanning, Y. Ko, and M. Staudacher, *Bethe Ansatz for Yangian Invariants: Towards Super Yang-Mills Scattering Amplitudes*, *Nucl.Phys.* **B883** (2014) 373, [arXiv:1312.1693].

[50] A. Amariti and D. Forcella, *Scattering Amplitudes and Toric Geometry*, *JHEP* **1309** (2013) 133, [arXiv:1305.5252].

[51] J. L. Bourjaily, S. Caron-Huot, and J. Trnka, *Dual-Conformal Regularization of Infrared Loop Divergences and the Chiral Box Expansion*, *ArXiv e-prints* (Mar., 2013) [arXiv:1303.4734].

[52] S. Caron-Huot, *Superconformal symmetry and two-loop amplitudes in planar N=4 super Yang-Mills*, *JHEP* **1112** (2011) 066, [arXiv:1105.5606].

[53] J. Drummond and L. Ferro, *The Yangian origin of the Grassmannian integral*, *JHEP* **1012** (2010) 010, [arXiv:1002.4622].

[54] N. Beisert, J. Henn, T. McLoughlin, and J. Plefka, *One-loop superconformal and Yangian symmetries of scattering amplitudes in mathcal{N} = 4 super Yang-Mills*, *Journal of High Energy Physics* **4** (Apr., 2010) 85, [arXiv:1002.1733].

[55] J. Drummond and L. Ferro, *Yangians, Grassmannians and T-duality*, *JHEP* **1007** (2010) 027, [arXiv:1001.3348].

[56] B. Feng, R. Huang, and Y. Jia, *Gauge Amplitude Identities by On-shell Recursion Relation in S-matrix Program*, *Phys.Lett.* **B695** (2011) 350–353, [arXiv:1004.3417].

[57] L. F. Alday, J. Maldacena, A. Sever, and P. Vieira, *Y-system for Scattering Amplitudes*, *J.Phys.* **A43** (2010) 485401, [arXiv:1002.2459].

[58] L. Mason and D. Skinner, *Dual Superconformal Invariance, Momentum Twistors and Grassmannians*, *JHEP* **0911** (2009) 045, [arXiv:0909.0250].

[59] N. Beisert, *T-Duality, Dual Conformal Symmetry and Integrability for Strings on AdS(5) x S**5*, *Fortsch.Phys.* **57** (2009) 329–337, [arXiv:0903.0609].

[60] A. Agarwal, N. Beisert, and T. McLoughlin, *Scattering in mass-deformed Script N= 4 Chern-Simons models*, *Journal of High Energy Physics* **6** (June, 2009) 45, [arXiv:0812.3367].

[61] T. Bargheer, N. Beisert, W. Galleas, F. Loebbert, and T. McLoughlin, *Exacting N=4 Superconformal Symmetry*, *JHEP* **0911** (2009) 056, [arXiv:0905.3738].

[62] I. Adam, A. Dekel, and Y. Oz, *On integrable backgrounds self-dual under fermionic T-duality*, *Journal of High Energy Physics* **4** (Apr., 2009) 120, [arXiv:0902.3805].

[63] H. Elvang and Y.-t. Huang, *Scattering Amplitudes*, arXiv:1308.1697.

[64] P. Benincasa, *New structures in scattering amplitudes: a review*, arXiv:1312.5583.

[65] N. Beisert, C. Ahn, L. F. Alday, Z. Bajnok, J. M. Drummond, L. Freyhult, N. Gromov, R. A. Janik, V. Kazakov, T. Klose, G. P. Korchemsky, C. Kristjansen, M. Magro, T. McLoughlin, J. A. Minahan, R. I. Nepomechie, A. Rej, R. Roiban, S. Schäfer-Nameki, C. Sieg, M. Staudacher, A. Torrielli, A. A. Tseytlin, P. Vieira, D. Volin, and K. Zoubos, *Review of AdS/CFT Integrability: An Overview*, *Letters in Mathematical Physics* **99** (Jan., 2012) 3–32, [arXiv:1012.3982].

[66] J. Drummond, *Tree-level amplitudes and dual superconformal symmetry*, *J.Phys.* **A44** (2011) 454010, [arXiv:1107.4544].

[67] L. J. Dixon, *Scattering amplitudes: the most perfect microscopic structures in the universe*, *J.Phys.* **A44** (2011) 454001, [arXiv:1105.0771].

[68] N. Beisert, *On Yangian Symmetry in Planar N=4 SYM*, arXiv:1004.5423.

[69] J. Bartels, L. Lipatov, and A. Prygarin, *Integrable spin chains and scattering amplitudes*, *J.Phys.* **A44** (2011) 454013, [arXiv:1104.0816].

[70] J. M. Henn, *Dual conformal symmetry at loop level: massive regularization*, *Journal of Physics A Mathematical General* **44** (Nov., 2011) 4011, [arXiv:1103.1016].

[71] T. Bargheer, N. Beisert, and F. Loebbert, *Exact superconformal and Yangian symmetry of scattering amplitudes*, *Journal of Physics A Mathematical General* **44** (Nov., 2011) 4012, [arXiv:1104.0700].

[72] R. Roiban, *Review of AdS/CFT Integrability, Chapter V.1: Scattering Amplitudes - a Brief Introduction*, *Lett.Math.Phys.* **99** (2012) 455–479, [arXiv:1012.4001].

[73] J. Drummond, *Review of AdS/CFT Integrability, Chapter V.2: Dual Superconformal Symmetry*, *Lett.Math.Phys.* **99** (2012) 481–505, [arXiv:1012.4002].

[74] N. J. Mackay, *Introduction to Yangian Symmetry in Integrable Field Theory*, *International Journal of Modern Physics A* **20** (2005) 7189–7217, [hep-th/0409183].

[75] D. Bernard, *An Introduction to Yangian Symmetries*, *International Journal of Modern Physics B* **7** (1993) 3517–3530, [hep-th/9211133].

[76] J. M. Henn and J. C. Plefka, *Scattering Amplitudes in Gauge Theories*, *Lect.Notes Phys.* **883** (2014).

[77] P. Du, G. Chen, and Y.-K. E. Cheung, *Permutation relations of generalized Yangian Invariants, unitarity cuts, and scattering amplitudes*, *JHEP* **1409** (2014) 115, [arXiv:1401.6610].

[78] A. Postnikov, *Total positivity, Grassmannians, and networks*, *ArXiv Mathematics e-prints* (Sept., 2006) [math/0609].

[79] R. Kleiss and H. Kuijf, *Multigluon cross sections and 5-jet production at hadron colliders*, *Nuclear Physics B* **312** (Jan., 1989) 616–644.

[80] I. M. Gelfand, R. M. Goresky, R. D. MacPherson, and V. V. Serganova, *Combinatorial geometries, convex polyhedra, and schubert cells*, *Advances in Mathematics* **63** (1987), no. 3 301–316.